J. Fluid Mech. (1994), *vol.* 258, *pp.* 131–165

On the linear stability of compressible plane Couette flow

By PETER W. DUCK,[1] GORDON ERLEBACHER[2] AND M. YOUSUFF HUSSAINI[2]

[1] Department of Mathematics, University of Manchester, Manchester, M13 9PL, UK

[2] Institute for Computer Applications in Science and Engineering, NASA Langley Research Center, Hampton, VA 23665, USA

(Received 29 July 1991 and in revised form 23 June 1993)

The linear stability of compressible plane Couette flow is investigated. The appropriate basic velocity and temperature distributions are perturbed by a small-amplitude normal-mode disturbance. The full small-amplitude disturbance equations are solved numerically at finite Reynolds numbers, and the inviscid limit of these equations is then investigated in some detail. It is found that instabilities can occur, although the corresponding growth rates are often quite small; the stability characteristics of the flow are quite different from unbounded flows. The effects of viscosity are also calculated, asymptotically, and shown to have a stabilizing role in all the cases investigated. Exceptional regimes to the problem occur when the wave speed of the disturbances approaches the velocity of either of the walls, and these regimes are also analysed in some detail. Finally, the effect of imposing radiation-type boundary conditions on the upper (moving) wall (in place of impermeability) is investigated, and shown to yield results common to both bounded and unbounded flows.

1. Introduction

Incompressible plane Couette flow possesses, perhaps, the simplest exact solution of the Navier–Stokes equations (see the remarks of Stewartson 1981), and (probably as a consequence) the study of the stability of this flow has been the subject of considerable attention over the years. Numerical studies of the linear stability problem have been carried out by Grohne (1954), Gallagher & Mercer (1962, 1964), Deardorff (1963), Davey (1973), and Gallagher (1974); however, none of these studies found evidence of instability. A number of analytic studies have also been carried out on this problem. Wasow (1953) showed that the flow is stable at all streamwise wavenumbers (α) if the Reynolds number (Re) is sufficiently large. The stability of the flow at low Reynolds number was demonstrated by Synge (1938). Dikii (1964) proved that all modes with wave speeds equal to the average of the wall velocities were stable and indeed that the imaginary component of the wave speed $\mathrm{Im}\{c\} < -\alpha/Re$. The first general proof of stability appears to be due to Romanov (1973) who showed that all normal modes of the linear problem are damped for $\alpha \geqslant 0$, $Re > 0$. Exact solutions of the Orr–Sommerfeld equations have been obtained by Reid (1979).

Another issue that has been studied is the question of a continuous spectrum. Case (1960, 1961) showed that the time-dependent inviscid problem has a continuous spectrum which decays in time as $1/t$, this spectrum arising as a direct consequence of the singularity of the inviscid equations at the critical layer, whilst Shivamoggi (1982) presented an example of a continuous spectrum which decayed exponentially in time.

A detailed analysis of modes for the large-Reynolds-number limit for general mean flows is given by Morawetz (1952), which has implications for plane Couette flow. She classified the modes into three sets. In the first set are eigenvalues which approach the inviscid eigenvalues in the limit of infinite Reynolds number. Since there are no discrete inviscid eigenvalues in the case of plane Couette flow, this first set is empty. In the second set, there is an infinity of eigensolutions unrelated to the inviscid problem, satisfying

$$|c-c_n| < \Delta(\alpha Re)^{-\frac{1}{2}}, \tag{1.1}$$

where Δ is a constant, and c_n is a root of

$$\mathrm{Im}\int_{y_1}^{y_2}[\mathrm{i}U_0(y)-c_n]^{\frac{1}{2}}\,\mathrm{d}y = \frac{n\pi}{2(\alpha Re)^{\frac{1}{2}}}, \tag{1.2}$$

where n is any integer, $U_0(y)$ is the velocity profile, α is the wavenumber, and the flow extends from $y = y_1$ to $y = y_2$. These modes are always stable (if Re is sufficiently large). In the third class are eigensolutions of the viscous problem that, as $\alpha Re \to \infty$, approach a finite V-shaped strip in c-space defined by one branch of

$$\mathrm{Re}\int_{y_c}^{y_1}[\mathrm{i}(U_0(y)-c)]^{\frac{1}{2}}\,\mathrm{d}y = 0, \tag{1.3}$$

and on branch of

$$\mathrm{Re}\int_{y_c}^{y_2}[\mathrm{i}(U_0(y)-c)]^{\frac{1}{2}}\,\mathrm{d}y = 0, \tag{1.4}$$

where $U_0(y_c) = \mathrm{Re}\{c\}$; these modes are either neutral or stable. Some generalizations for compressible flow can be found in Morawetz (1954).

However, there is a dichotomy between the theoretical and computational results described above and experimental results at large Reynolds numbers, in which instabilities are certainly observed (Taylor 1936; Reichardt 1956; Robertson 1959). A number of attempts have been made to explain this through the inclusion of nonlinear terms. Investigations of this type include the work of Watson (1960), Eckhaus (1965), Hains (1967), Reynolds & Potter (1967), Ellingsen, Gjevik & Palm (1970), and Lessen & Cheifetz (1975). These studies used several techniques involving various degrees of mathematical rigour, and led to a number of conclusions (some partly contradictory), although on balance the evidence was that finite-amplitude effects could, indeed, destabilize the flow. Additionally, Romanov (1973) considered the nonlinear initial-value problem and showed that there is a unique solution which is asymptotically stable if the norm of the initial disturbances in Sobolev space is sufficiently small.

The linear stability of compressible flows is considerably less well understood than corresponding incompressible flows. Most of the work (which has for the most part been based on the parallel mean flow assumption) has been with regard to boundary-layer flows (e.g. Lees & Lin 1946; Mack 1963, 1965*a*, *b*, 1969, 1984, 1987, 1990; Reshotko 1962, 1976) and more recently to jets with shear layers (e.g. Tam & Hu 1989*a*, *b*; Greenough *et al.* 1988; Papageorgiou 1990; Jackson & Grosch 1989; Mack 1990). Other, more recent, related work, with particular emphasis on the hypersonic limit of the stability problem, is that of Cowley & Hall (1990), Smith & Brown (1990), Goldstein & Wundrow (1990), Balsa & Goldstein (1990), and Blackaby, Cowley & Hall (1993). Interestingly, a general feature of hypersonic flow stability is a trend towards less unstable flows. Nonlinear critical-layer analysis of compressible flows has also been considered by Gajjar & Cole (1989) and Gajjar (1990).

The first (of a number) of distinguishing features of the stability of compressible flows was found by Lees & Lin (1946). This relates to the replacement of the (classical) inflexion-point condition in the streamwise velocity profile (for the existence of neutral inviscid modes), by the generalized-inflexion-point (GIP) condition which involves the mean density distribution also. This condition relates to the existence of neutral 'inviscid' modes (i.e. modes of wavelength comparable to the characteristic scales of the mean flow, for example the displacement thickness in the case of boundary-layer flows, or lateral extent in the case of confined flows).

In addition to these 'subsonic' modes associated with the GIP, there may also exist supersonic neutral modes (Mack 1963, 1965*a*, *b*, 1969, 1984, 1987, 1990), and subsonic modes not associated with a GIP can become unstable in the presence of a relative supersonic pocket between the wall and the relative sonic line (where the perturbation wave is propagating sonically relative to the mean flow). However, to date, a simple mechanism that explains why and precisely under what conditions these types of mode exist has yet to be propounded. Some general remarks concerning stability at large Reynolds numbers have been made, however, by Lin (1955). In the case of stable disturbances, with finite damping, it was shown that a finite viscous region in the interior of the fluid exists for arbitrarily large Reynolds number. In the case of unstable disturbances, with finite amplification, there is no inner viscous region if the Reynolds number of the mean flow is large enough. In the case of neutral disturbances (for constant Prandtl number) it was rigorously shown that if a viscous region does exist, its width shrinks to zero with an increase in Reynolds number. Studies relating to the stability of other classes of compressible flow include the work of Tam & Hu (1989*a*, *b*), Greenough *et al.* (1989), Zhuang, Kubota & Dimotakis (1990) (confined two-dimensional supersonic mixing layers), Macaraeg & Streett (1989), and Mack (1990) (compressible mixing layers).

The object of this study is to analyse some of the characteristics of compressible plane Couette flow. Although analytic expressions for the mean streamwise velocity $U_0(y)$ and temperature $T_0(y)$ are not available for general viscosity laws, $T_0(y)$ may be expressed as a second-order polynomial in $U_0(y)$, and hence it is relatively straightforward to generate mean flow profiles, under different conditions. Thus this profile represents a rare opportunity to analyse an *exact* solution of the full equations of motion and energy without the need for other approximations (notably the parallel-flow approximation). Some work has previously been carried out to investigate the compressible stability of plane Couette flow. Glatzel (1988) considered inviscid stability of this problem, and then Glatzel (1989) went on to incorporate the effects of viscosity. However, both these works were for the special case of constant viscosity, density and pressure (implying constant temperature also), which led to a fourth-order system (rather than a sixth-order system). Girard (1988) considered the same problem, and also assumed constant viscosity (although he did allow for variations in density and temperature). In this paper, we choose to consider the stability of the mean flow profile described above, which is a correct and proper solution of the full compressible Navier–Stokes equations. We show that the details of the mean flow profile have a profound effect on the stability of the flow.

The layout of the paper is as follows. In §2 we formulate the problem, stating our fundamental assumptions and equations of motion. In §3 we derive the equations of motion for the basic flow, in which the problem is reduced to that of a straightforward, although nonlinear, first-order system that may be solved by means of standard numerical means. In §4 we derive the (full) small-amplitude disturbance equations, neglecting only terms in perturbation amplitude squared, and we describe a numerical

scheme to treat this system, together with a number of numerical results. In §5 we consider the inviscid limit of these equations; we show how the so-called 'generalized inflexion point' is relevant in this context, and under what circumstances we can expect such a point to occur with our basic profile.

Numerical results for the inviscid problem are presented in §6, and, most importantly, it is shown that unstable modes are possible, although according to inviscid theory there are many regions where many modes are neutrally stable. These neutral modes are investigated further in §7, in which the effects of viscosity are included, and shown to always have a stabilizing role for high Reynolds numbers. However, this study also raises important questions regarding the applicability of our results, in particular in regions of changeover from the neutral to non-neutral state. This region is investigated in some detail in §8. Because of the apparent discrepancy in results between bounded and unbounded stability analyses, in §9 we consider a change in boundary conditions on the upper (moving) wall, from one of impermeability to one of radiation. Finally, in §10 we present some conclusions.

2. Formulation

We assume that we have a compressible Newtonian perfect fluid between two infinite parallel planes defined by $y^* = 0$ and $y^* = h$. The x^*-axis is taken to lie in the plane of the lower wall. We take the fluid to have density ρ^*, viscosity μ^*, and second coefficient of viscosity ζ^* (which may be taken to be zero for a monatomic gas). The upper wall has velocity U_∞ (a subscript ∞ refers to unperturbed conditions on the upper wall), taken parallel to the plane of the wall, while the lower wall is at rest. Although the basic flow will be taken to be one-dimensional, later we shall consider two-dimensional perturbations of this flow. The velocity components are taken to be $\boldsymbol{u}^* = (u^*, v^*)$ in the x^*- and y^*-directions respectively, and the pressure and temperature are written as p^* and T^* respectively. We non-dimensionalize velocities with respect to U_∞, lengthscales with respect to h, density with respect to ρ^*_∞, viscosity with respect to μ^*_∞, temperature with respect to T^*_∞ and pressure with respect to $\rho^*_\infty R^* T^*_\infty$, where the gas constant $R^* = C_p - C_v$, and C_p and C_v are the specific heats at constant pressure and volume respectively; non-dimensional quantities are denoted using the same notation as corresponding dimensional quantities, except without the superscript asterisk.

The continuity equation may then be written

$$\frac{\partial \rho}{\partial t} + \frac{\partial}{\partial x}(\rho u) + \frac{\partial}{\partial y}(\rho v) = 0. \tag{2.1}$$

Here, and throughout the paper, we assume that the appropriate dimensional timescale is $O(h/U_\infty)$.

The momentum equations are written

$$\rho\left[\frac{\partial u}{\partial t} + u\frac{\partial u}{\partial x} + v\frac{\partial u}{\partial y}\right] = -\frac{1}{\gamma M_\infty^2}\frac{\partial p}{\partial x} + \frac{1}{Re}\left\{\frac{\partial}{\partial x}\left[2\mu\frac{\partial u}{\partial x} + \lambda \nabla \cdot \boldsymbol{u}\right] + \frac{\partial}{\partial y}\left[\mu\left(\frac{\partial u}{\partial y} + \frac{\partial v}{\partial x}\right)\right]\right\}, \tag{2.2}$$

$$\rho\left[\frac{\partial v}{\partial t} + u\frac{\partial v}{\partial x} + v\frac{\partial v}{\partial y}\right] = -\frac{1}{\gamma M_\infty^2}\frac{\partial p}{\partial y} + \frac{1}{Re}\left\{\frac{\partial}{\partial y}\left[2\mu\frac{\partial v}{\partial y} + \lambda \nabla \cdot \boldsymbol{u}\right] + \frac{\partial}{\partial x}\left[\mu\left(\frac{\partial u}{\partial y} + \frac{\partial v}{\partial x}\right)\right]\right\}. \tag{2.3}$$

Here the Reynolds number Re is defined by

$$Re = U_\infty \rho^*_\infty h/\mu^*_\infty, \tag{2.4}$$

the Mach number M_∞ by

$$M_\infty = U_\infty/(\gamma R^* T_\infty^*)^{\frac{1}{2}}, \tag{2.5}$$

and the ratio of specific heats by γ.

The non-dimensional form of the energy equation used is

$$\rho\left[\frac{\partial T}{\partial t}+u\frac{\partial T}{\partial x}+v\frac{\partial T}{\partial y}\right]-\left(\frac{\gamma-1}{\gamma}\right)\left[\frac{\partial p}{\partial t}+u\frac{\partial p}{\partial x}+v\frac{\partial p}{\partial y}\right]=\frac{1}{Re}\left\{\frac{\partial}{\partial y}\left[\mu\frac{\partial T}{\partial y}\right]+\frac{\partial}{\partial x}\left[\frac{\mu}{\sigma}\frac{\partial T}{\partial x}\right]\right\}$$
$$+\frac{2\mu(\gamma-1)M_\infty^2}{Re}\left[\left(\frac{\partial u}{\partial x}\right)^2+\left(\frac{\partial v}{\partial y}\right)^2+\frac{1}{2}\left(\frac{\partial u}{\partial y}+\frac{\partial v}{\partial x}\right)^2+\frac{\lambda}{2\mu}\left(\frac{\partial u}{\partial x}+\frac{\partial v}{\partial y}\right)^2\right]. \tag{2.6}$$

Here σ is the Prandtl number $\sigma = \mu^* C_p/K^*$, (2.7)

where K^* is the coefficient of heat conductivity. The equation of state is simply

$$p = \rho T. \tag{2.8}$$

We assume that viscosity depends solely on temperature, and in particular we assume Sutherland's law

$$\mu = T^{\frac{3}{2}}\left(\frac{1+C}{T+C}\right), \tag{2.9}$$

where C is a constant. Finally, $\lambda = \zeta - 2/3\mu$ and the Stokes assumption $\zeta = 0$ is assumed throughout the paper.

In the following section we consider the basic flow which we expect to depend on y only.

3. Compressible Couette flow

We seek a solution of (2.1)–(2.6) which is dependent on y only, together with a constant mean pressure. By continuity we must have $v = 0$. We then seek a solution of the form

$$u = U_0(y), \quad T = T_0(y), \quad \mu = \mu_0(y). \tag{3.1}$$

We then have

$$(\mu_0 U_{0y})_y = 0, \tag{3.2}$$

$$\left[\frac{\mu_0 T_{0y}}{\sigma}\right]_y + (\gamma-1)M_\infty^2 \mu_0 (U_{0y})^2 = 0, \tag{3.3}$$

subject to

$$\left.\begin{aligned} U_0(0) = 0, U_0(1) = 1, \\ T_0(0) = T_w, \quad T_0 = 1. \end{aligned}\right\} \tag{3.4}$$

It follows immediately from (3.2) that the shear stress τ is a constant through the profile, i.e.

$$\tau = \mu_0 U_{0y} = \text{constant}. \tag{3.5}$$

The energy equation may then be written as

$$\left[\frac{\mu_0}{\sigma} T_{0y} + (\gamma-1)M_\infty^2 U_0 \tau\right]_y = 0. \tag{3.6}$$

It is easy to show, using (3.6) that the recovery temperature (i.e. the wall temperature with adiabatic conditions) is

$$T_r = 1 + \tfrac{1}{2}(\gamma-1)\sigma M_\infty^2, \tag{3.7}$$

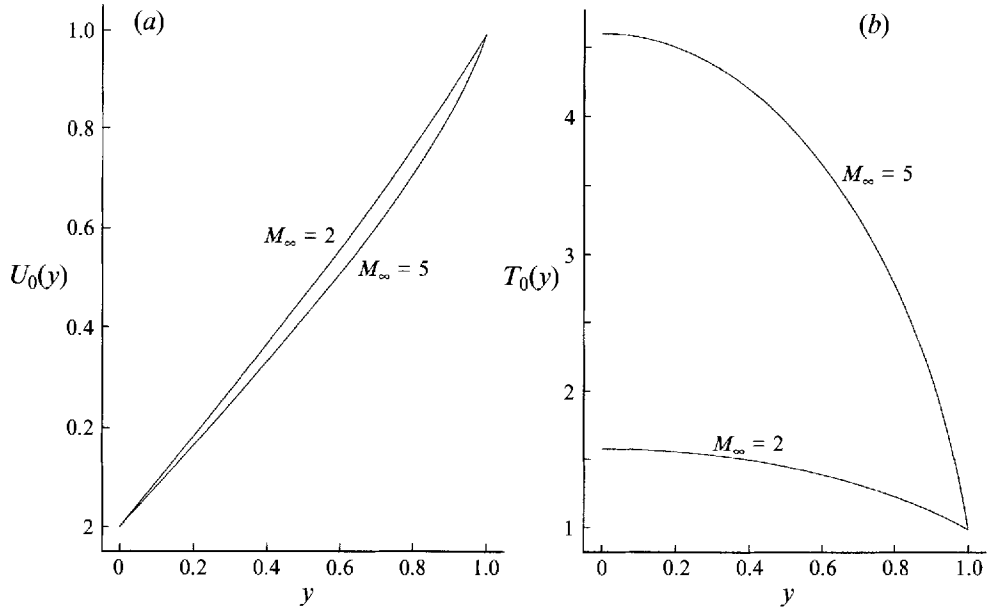

FIGURE 1. Basic flow, adiabatic case, $M_\infty = 2, 5$. (*a*) $U_0(y)$, (*b*) $T_0(y)$.

and we define the recovery factor

$$r = T_w/T_r. \tag{3.8}$$

Equation (3.6) may be integrated and written in the form

$$T_0 = T_r\left\{r+(1-r)\,U_0-\left(1-\frac{1}{T_r}\right)U_0^2\right\}. \tag{3.9}$$

Equations (3.5) and (3.9), together with an appropriate viscosity law (we used (2.9)) and boundary conditions (3.4), then completely determine the problem; τ is unknown *a priori* and must therefore be determined as part of an iterative process. The mean pressure profile is constant. The process was then to guess a value of τ, and then to use a fourth-order Runge–Kutta scheme to generate the solution (using (3.5)) from $y = 0$ to $y = 1$, where the condition on $U_0(y)$ will not be satisfied. This condition, in conjunction with a Newton iteration procedure, was then used to update the value of τ. This scheme was then repeated until convergence of τ had been achieved.

Results for the basic flow are shown in figure 1(*a*) ($U_0(y)$) and figure 1(*b*) ($T_0(y)$), at the two Mach numbers to be studied throughout this paper ($M_\infty = 2$ and 5) for an adiabatic lower wall. We set $\gamma = 1.4$, $\sigma = 0.72$, together with the Sutherland constant $C = 0.5$. These results show that there is a (mild) deviation away from the uniform shear solution for $U_0(y)$, whilst there is a (dramatic) deviation of $T_0(y)$ from the uniform state of incompressible theory.

4. The small-amplitude disturbance equations

Here we take the solution to be that of Couette flow (as discussed in the previous section) together with a small-amplitude perturbation. More specifically, we write

$$\left.\begin{aligned} u &= U_0(y)+\delta\tilde{u}(y)\,E+O(\delta^2), & v &= \delta\alpha\tilde{v}(y)\,E+O(\delta^2),\\ p &= 1+\delta\tilde{p}(y)\,E+O(\delta^2), & \rho &= \rho_0(y)+\delta\tilde{\rho}(y)\,E+O(\delta^2),\\ \mu &= \mu_0(y)+\delta\tilde{\mu}(y)\,E+O(\delta^2), & \zeta &= \zeta_0(y)+\delta\tilde{\zeta}(y)\,E+O(\delta^2),\\ T &= T_0(y)+\delta\tilde{T}(y)\,E+O(\delta^2), \end{aligned}\right\} \tag{4.1}$$

where
$$E = \exp[\mathrm{i}\alpha(x-ct)], \tag{4.2}$$

and δ is the (small) amplitude of the perturbation. If we take terms $O(\delta)$ in (2.1)–(2.3), (2.6) we obtain the following full, small-disturbance equations:

$$-\mathrm{i}c\tilde{\rho}+\mathrm{i}\rho_0\tilde{u}+\mathrm{i}U_0\tilde{\rho}+\tilde{v}\rho_{0y}+\rho_0\tilde{v}_y = 0, \tag{4.3}$$

$$\rho_0[-\mathrm{i}\alpha c\tilde{u}+\mathrm{i}\alpha U_0\tilde{u}+\alpha\tilde{v}U_{0y}]+\frac{\mathrm{i}\alpha}{\gamma M_\infty^2}\tilde{p}$$
$$= \frac{1}{Re}\{-2\mu_0\alpha^2\tilde{u}+\lambda_0[-\alpha^2\tilde{u}+\mathrm{i}\alpha\tilde{v}_y]+\mu_{0y}[\tilde{u}_y+\mathrm{i}\alpha\tilde{v}]+\mu_0[\tilde{u}_{yy}+\mathrm{i}\alpha\tilde{v}_y]+\tilde{\mu}_y U_{0y}+\tilde{\mu}U_{0yy}\}, \tag{4.4}$$

$$\rho_0[-\mathrm{i}\alpha^2\tilde{v}+\mathrm{i}\alpha^2U_0\tilde{v}]+\frac{\tilde{p}_y}{\gamma M_\infty^2}$$
$$= \frac{1}{Re}\{2\mu_{0y}\tilde{v}_y+2\mu_0\tilde{v}_{yy}+\lambda_{0y}(\mathrm{i}\alpha\tilde{u}+\tilde{v}_y)+\lambda_0(\mathrm{i}\alpha\tilde{u}_y+\tilde{v}_{yy})+\mu_0(\mathrm{i}\alpha\tilde{u}_y-\alpha^2\tilde{v})+\mathrm{i}\alpha\tilde{\mu}U_{0y}\}, \tag{4.5}$$

$$\rho_0[-\mathrm{i}\alpha c\tilde{T}+\mathrm{i}\alpha U_0\tilde{T}+\alpha\tilde{v}T_{0y}]-\left(\frac{\gamma-1}{\gamma}\right)[-\mathrm{i}\alpha c\tilde{p}+\mathrm{i}\alpha U_0\tilde{p}]$$
$$= \frac{1}{\sigma Re}\{\mu_0\tilde{T}_{yy}+\mu_{0y}\tilde{T}_y+\mu\tilde{T}_{0yy}+\tilde{\mu}_y T_{0y}-\alpha^2\mu_0\tilde{T}\}$$
$$+\frac{(\gamma-1)M_\infty^2}{Re}\{\mu_0 U_{0y}\tilde{u}_y+\tilde{\mu}(U_{0y})^2+2\mu_0\mathrm{i}\alpha U_{0y}\tilde{v}\}. \tag{4.6}$$

The perturbation equation of state is then

$$\tilde{p} = T_0\tilde{\rho}+\tilde{T}/T_0. \tag{4.7}$$

No-slip and impermeability conditions are applied to the velocity perturbations at both walls, namely

$$\tilde{u}(0) = \tilde{u}(1) = \tilde{v}(0) = \tilde{v}(1) = 0. \tag{4.8}$$

The temperature boundary conditions are $\tilde{T}(1) = 0$, while on the lower wall,

$$\tilde{T}(0) = 0 \tag{4.9}$$

for a heated/cooled surface and

$$\frac{\partial\tilde{T}}{\partial y} = 0 \quad \text{on} \quad y = 0 \tag{4.10}$$

for an insulated wall.

We now present results based on the full set of viscous compressible linearized equations, i.e. (4.3)–(4.7) above.

The stability results are obtained from a spectral temporal linear stability code written by Herbert (1990). The code assumes a global representation of all variables in appropriate basis functions which can vary from variable to variable. The basis functions for the velocity components satisfy the imposed boundary conditions. Velocity perturbations are set to zero at $y = 0$ and $y = 1$. Thus, the velocity basis functions are linear combinations of Chebyshev polynomials. In terms of the Chebyshev polynomials $T_n(\tilde{y})$, these basis functions are defined as

$$U_n(y) = T_{n+2}(\tilde{y})-T_n(\tilde{y}), \tag{4.11}$$

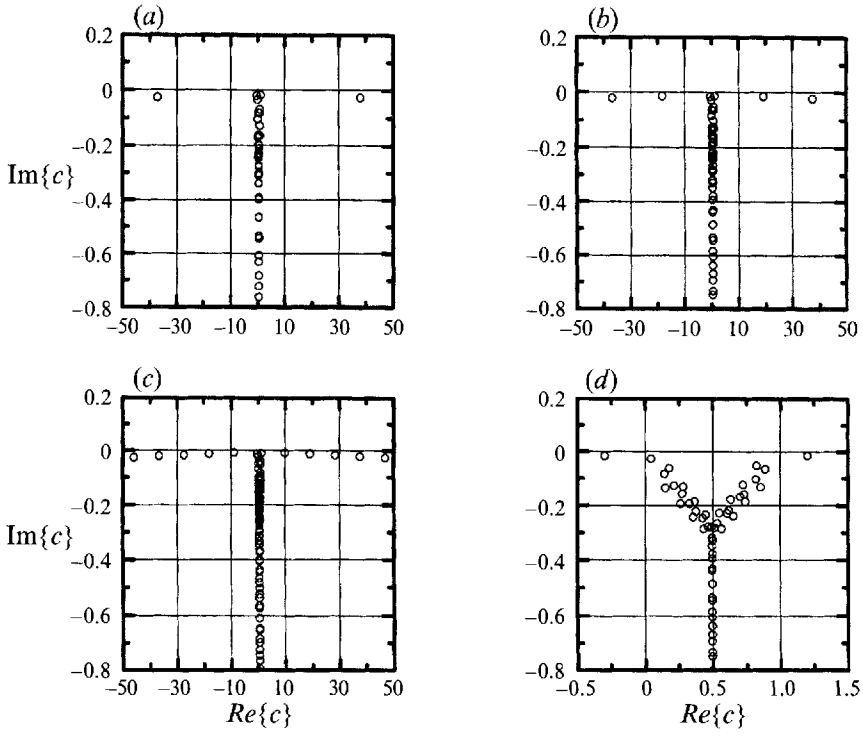

FIGURE 2. Spectrum at $M_\infty = 2$, $Re = 2 \times 10^5$, at 100 collocation points. (*a*) $\alpha = 0.05$, (*b*) $\alpha = 0.10$, (*c*) $\alpha = 0.20$, and (*d*) blowup of (*b*).

where $\tilde{y} = 2y - 1$. Boundary conditions for the density and temperature perturbation waves are of more general nature, so these variables are represented as a standard Chebyshev series. In this section, only adiabatic results are shown. Thus, the y-derivative of the temperature perturbation is zero at the lower wall. The upper wall is insulated; therefore the temperature perturbation is set to zero. The density at the walls is obtained by integration of the continuity equation.

The numerical algorithm is based on an expansion of the unknown variables in terms of known basis functions. Taking the perturbation density ($\tilde{\rho}$) as an example, let

$$\tilde{\rho}(y) = \sum_n a_n T_n(\tilde{y}), \tag{4.12}$$

and its first derivative

$$\frac{\mathrm{d}\tilde{\rho}(\tilde{y})}{\mathrm{d}y} = \sum_n a_n \frac{\mathrm{d}T_n(\tilde{y})}{\mathrm{d}y} \tag{4.13}$$

be evaluated at each collocation point. Inserting $\tilde{\rho}$ and the other variables into the linearized stability equations leads to a system of linear equations for the coefficients of the basis functions. From these one can either calculate a global spectrum using routines from the IMSL library or obtain a single eigenvalue at a sequence of parameter values using a continuation technique. Details are given in Herbert (1990).

Figures 2 and 3 correspond to $M_\infty = 2$. The dependence of the eigenvalue of inviscid character (i.e. those eigenvalues close to $\mathrm{Im}\{c\} = 0$, which in this case also tend to be relatively isolated from their neighbours) is shown in figures 2(*a*)–2(*c*) which correspond to $\alpha = 0.05$, 0.10 and 0.20 respectively, all at $Re = 2 \times 10^5$, and obtained with 100 collocation points. It is clear from the sequence of figures that one inviscid

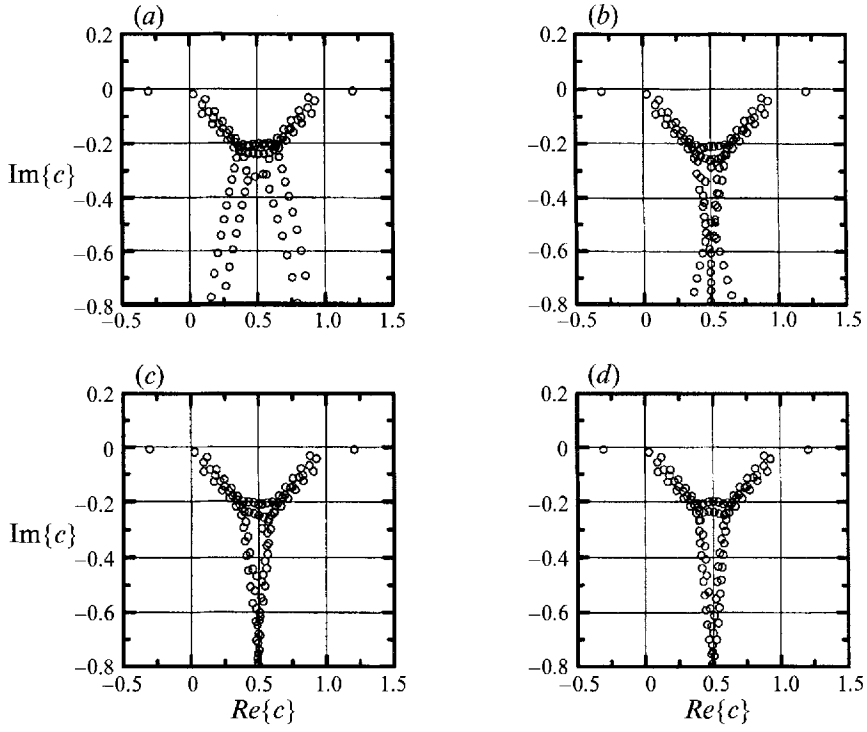

FIGURE 3. Phase velocity spectrum at $M_\infty = 2$, $\alpha = 0.1$, $Re = 7 \times 10^5$. (*a*) 75 collocation points, (*b*) 100, (*c*) 125, (*d*) 150.

eigenvalue is approximately stationary, while the remaining inviscid eigenvalues originate from very large values of $\mathrm{Re}\{c\}$ at very low α. A magnification of figure 2(*b*) (shown in figure 2*d*) shows the region of the spectrum corresponding to $0 < \mathrm{Re}\{c\} < 1$. One notes the general 'Y' shape of the spectrum as discussed by Morawetz (1952, 1954). The spectrum is composed of three 'Y' shaped pieces. These are due to the structure of the viscous terms of the two momentum equations and the temperature equation. The coupling between the equations and the non-unit Prandtl number leads to the non-superposition of the 'Y' singular curves as $Re \to \infty$. Before drawing any general conclusions however, we show spectra at $Re = 7 \times 10^5$ in figure 3, leaving all other parameters unchanged with respect to figure 2. As expected, higher resolution is required to properly resolve the spectrum. The sequence of figures 3(*a*)–(*d*) correspond to resolutions of 75, 100, 125 and 150 collocation points respectively. Although Morawetz (1952) predicts that there is a set of 'viscous' eigenvalues which lie on the edges of the 'V' part of the 'Y', packed with a density proportional to $(\alpha Re)^{\frac{1}{2}}$, it is clear that at $M_\infty = 2$, the triple point of the 'Y' is cut off by two horizontal bands of eigenvalues. The word horizontal is used here as a qualitative description. At the lower resolution of $N = 75$, the bands are slightly wider than for higher N. It is not completely clear whether these bands will remain or disappear as $N \to \infty$. A definitive answer would require further investigation into the properties of the viscous component of the spectrum at high Reynolds numbers and high Mach numbers. Comparing figures 3(*b*) and 3(*d*), it is clear that one effect of insufficient resolution is the splitting of the spectrum from the vertical part at the bottom of the 'Y'. However, such a splitting is not *always* indicative of loss of resolution (see figure 4 at $\alpha = 0.1$, $M_\infty = 5$, $Re = 2 \times 10^6$).

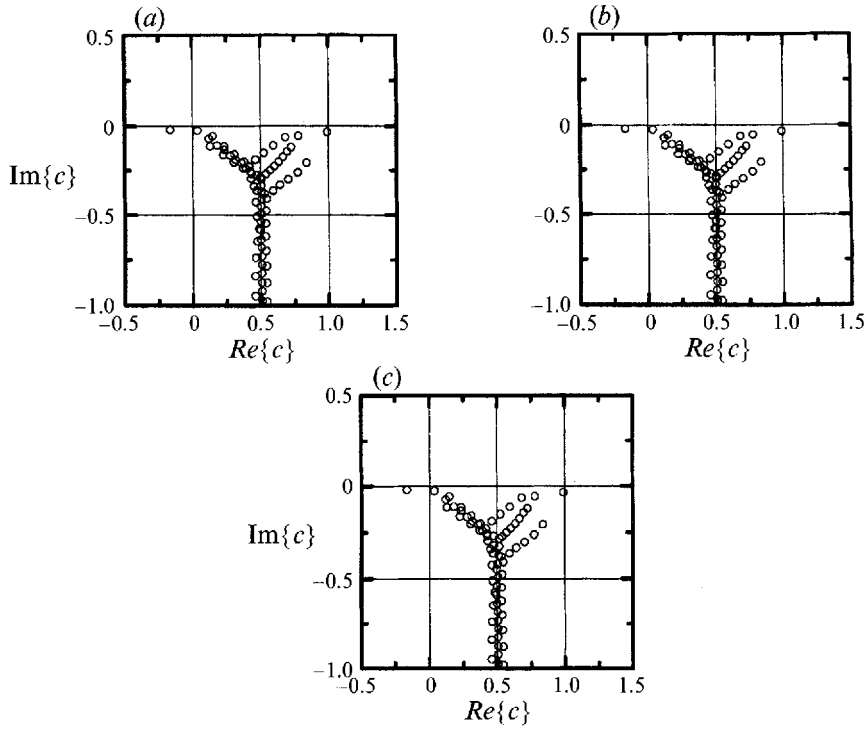

FIGURE 4. Phase velocity spectrum at $M_\infty = 5$, $\alpha = 0.1$, $Re = 2 \times 10^6$. (*a*) 100 collocation points, (*b*) 125, (*c*) 150.

We now turn our attention to a similar set of spectra at $M_\infty = 5$ which seem to exhibit a more complex character than their $M_\infty = 2$ counterparts. At $Re = 2 \times 10^6$, $\alpha = 0.1$, the three 'Y' shaped curves are clearly present (figure 4). These structures subsist in an unmodified form (i.e. without the horizontal bands) at higher Reynolds numbers at the higher M_∞. One 'Y' is approximately symmetrical about the $\mathrm{Re}\{c\} = 0.5$ axis. The vertical part of the 'Y' has split into three pieces, one along $\mathrm{Re}\{c\} = 0.5$, and the other two curves placed symmetrically about $\mathrm{Re}\{c\} = 0.5$. The actual locus of points along these curves shows a similarity with the continuous temporal boundary-layer spectra discussed in Ashpis & Erlebacher (1990). As the Reynolds number is increased to 5×10^6, the resolution requirements simultaneously increase (figure 5). Only when the vertical locus of eigenvalues along $\mathrm{Re}\{c\} = 0.5$ appears, is the resolution adequate, at least for the part of the spectra above it, although this statement is not quite true near the horizontal bands. The unchanging vertical position of these bands as N increases from 125 to 150 indicates that their presence is not an artifact of a loss of resolution.

To complete the picture, figure 6 shows the spectrum at $M_\infty = 5$, $\alpha = 3.5$ and $Re = 2 \times 10^5$. Now, several inviscid modes have moved into the $0 < \mathrm{Re}\{c\} < 1$ range. As each mode crosses $\mathrm{Re}\{c\} = 0$ or $\mathrm{Re}\{c\} = 1$ regions, a critical layer develops; this is examined in §6. Once again, as the Reynolds number increased, the width of the horizontal bands increases, and resolution studies indicate that they do not disappear as $N \to \infty$.

From these spectra, it is clear that it is somewhat difficult to judge the convergence of particular eigenmodes. A general rule of thumb states that the least-stable eigenvalues converge the fastest with increasing resolution. However, this should not

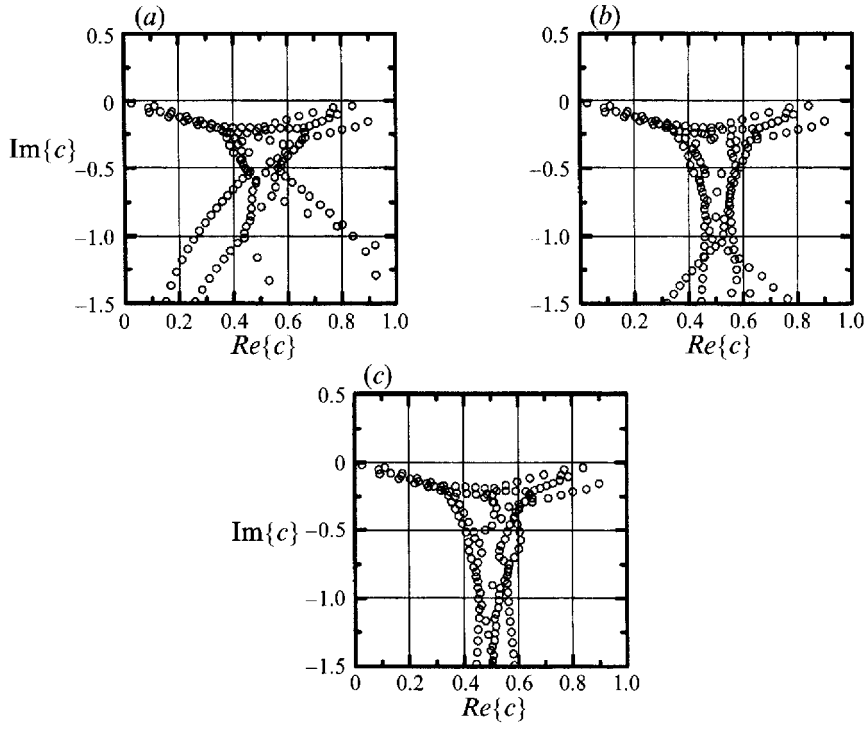

FIGURE 5. Phase velocity spectrum at $M_\infty = 5$, $\alpha = 0.1$, $Re = 5 \times 10^6$. (*a*) 100 collocation points, (*b*) 125, (*c*) 150.

be taken for granted. Recent work by Reddy, Schmid & Henningson (1993) conclusively demonstrates that certain regions of the spectra are *very* sensitive to very small (random) perturbations of the linear matrix elements. Perturbations on the order of 10^{-6} are sometimes sufficient to visually displace the eigenvalues. In most cases, the modes in the neighbourhood of the triple point of the 'Y' are the most sensitive. Since the matrix elements must change with increasing resolution, it is clear that certain modes will never converge, however accurately the computation is accomplished.

Some comments are in order concerning our choice of an adiabatic fluctuating temperature boundary condition at the wall. We have computed several spectra with the zero perturbation temperature at the wall (high-frequency limit). The only changes in the spectra occurred in one of the left branches of the 'Y'. This branch corresponds specifically to the conductive temperature modes. Changing the temperature boundary condition at the wall simply shifts that branch parallel to itself by approximately half a wavelength (spacing between two successive modes along the branch). This result can be obtained by considering a WKB approximation of the energy equation in the limit of high Reynolds number. Since the modes we are considering in this paper have an inviscid limit, and are therefore not on those branches, the change of boundary conditions does not affect the conclusions of this paper.

In anticipation of the results presented in the following sections, we plot in figure 7(*a*) the evolution of the mode II phase velocity (finite $\mathrm{Re}\{c\}$ as $\alpha \to 0$) as a function of α. This is carried out for several resolutions and at two different Reynolds numbers. Although inviscid theory suggests stronger instabilities at $M = 5$, viscous calculations indicate that the resolution requirements become much more severe. We therefore restrict ourselves to $M_\infty = 2$, and $Re = 7 \times 10^5$ and 1.4×10^6. Figure 7(*b*) shows that

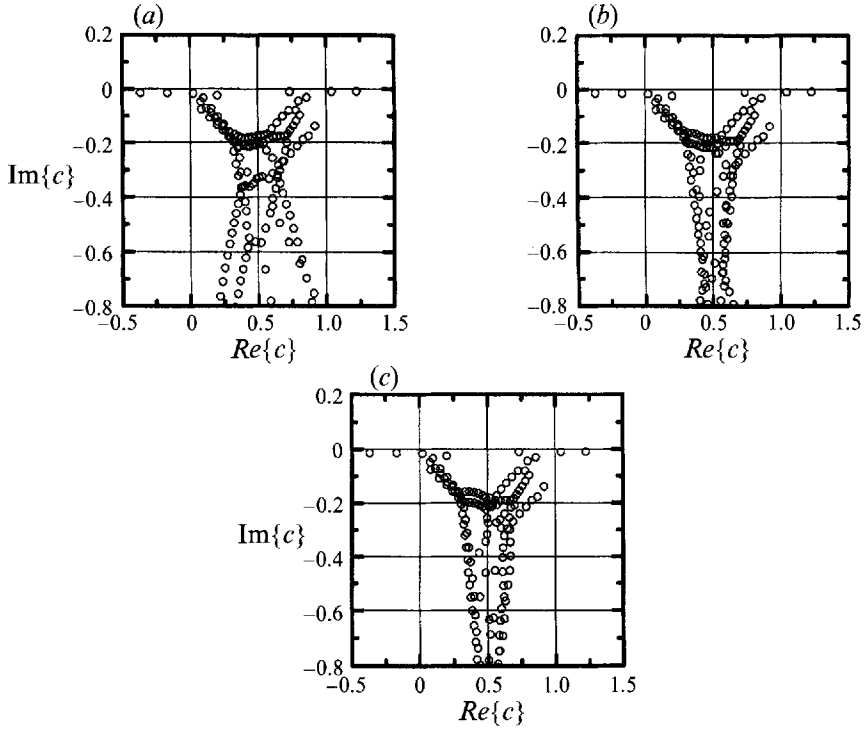

FIGURE 6. Phase velocity spectrum at $M_\infty = 5$, $\alpha = 3.5$, $Re = 2 \times 10^5$. (*a*) 100 collocation points, (*b*) 125, (*c*) 150.

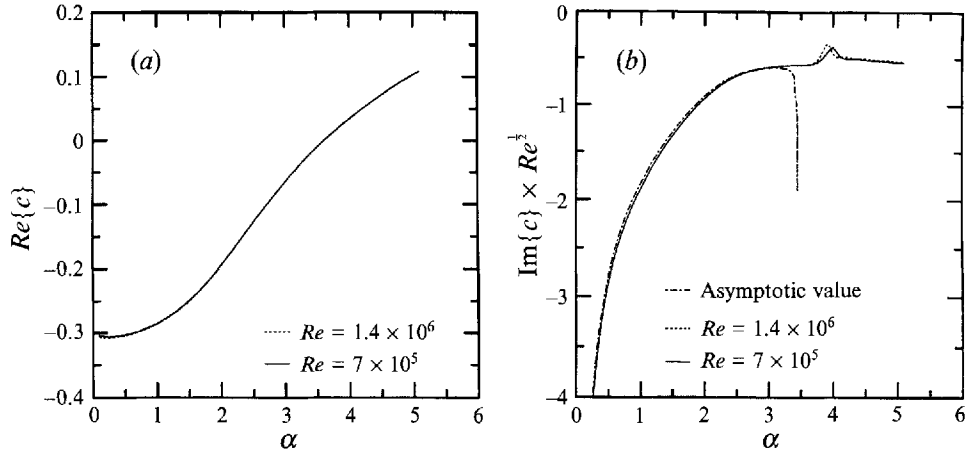

FIGURE 7. (*a*) $Re\{c\}$ as a function of α for $M_\infty = 2$ (mode II), at $Re = 7 \times 10^5$ and $Re = 1.4 \times 10^6$. (*b*) $\mathrm{Im}\{c\}\, Re^{\frac{1}{2}}$ as a function of α for $M_\infty = 2$ (mode II), at $Re = 7 \times 10^5$ and $Re = 1.4 \times 10^6$. The third curve is $\mathrm{Im}\{c_1\}$ obtained from asymptotic theory.

$\mathrm{Im}\{c\}$ exhibits a local maximum near $\alpha = 4$. This mode becomes less stable at higher Re, while α shifts to a slightly lower value. As expected, a higher resolution is required at $Re = 1.4 \times 10^6$ ($N = 150$), as opposed to $N = 100$ at $Re = 7 \times 10^5$. Unfortunately, we are not able to increase Re beyond 1.4×10^6 and still obtain accurate results at

resolutions not exceeding $N = 150$. Further discussion of figure 7(*b*) is deferred until the asymptotic theory at large Re has been presented.

In the following sections, we examine solutions of the stability problem in the limit $Re \to \infty$. Guided by a number of previous viscous theories, together with the work of Morawetz (1952, 1954), we expect, in general, the solution to develop in the form

$$\left.\begin{aligned} \tilde{u} &= \tilde{u}_0(y) + Re^{-\frac{1}{2}}\tilde{u}_1(y) + O(Re^{-1}), \\ \tilde{v} &= \tilde{v}_0(y) + Re^{-\frac{1}{2}}\tilde{v}_1(y) + O(Re^{-1}), \\ \tilde{T} &= \tilde{T}_0(y) + Re^{-\frac{1}{2}}\tilde{T}_1(y) + O(Re^{-1}), \\ \tilde{p} &= \tilde{P}_0(y) + Re^{-\frac{1}{2}}\tilde{P}_1(y) + O(Re^{-1}), \\ c &= c_0 + Re^{-\frac{1}{2}}c_1 + O(Re^{-1}). \end{aligned}\right\} \tag{4.14}$$

5. Inviscid disturbance equations

Taking equations (4.3)–(4.7), and then retaining lowest-order terms in Re (see Mack 1984, for example), we obtain the following two first-order equations for the leading-order normal velocity ($\tilde{v} = \tilde{v}_0$) and pressure ($\tilde{p} = \tilde{p}_0$) perturbations respectively:

$$\tilde{v}_{0y} - \frac{U_{0y}\tilde{v}_0}{U_0 - c_0} = \frac{\mathrm{i}\tilde{p}_0}{\gamma M_\infty^2}\frac{\{T_0 - M_\infty^2(U_0 - c_0)^2\}}{U_0 - c_0}, \tag{5.1}$$

$$\frac{\tilde{p}_{0y}}{\gamma M_\infty^2} = -\frac{\mathrm{i}\alpha^2}{T_0}(U_0 - c_0)\tilde{v}_0, \tag{5.2}$$

where the appropriate boundary conditions to be applied to this system are

$$\tilde{v}_0(0) = \tilde{v}_0(1) = 0, \tag{5.3}$$

implying

$$\tilde{p}_{0y}(0) = \tilde{p}_{0y}(1) = 0, \tag{5.4}$$

where c_0 is the complex wave speed of this system. Equations (5.1) and (5.2) may be combined to yield the single second-order equation (see for example Mack 1984, 1987)

$$\frac{\mathrm{d}}{\mathrm{d}y}\left\{\frac{(U_0 - c_0)\tilde{v}_{0y} - U_{0y}\tilde{v}_0}{T_0 - M_\infty^2(U_0 - c_0)^2}\right\} = \alpha^2\frac{(U_0 - c_0)}{T_0}\tilde{v}_0 \tag{5.5}$$

for $\tilde{v}_0$.

Before investigating any of the above systems numerically, it is interesting to study the significance of so-called 'generalized inflexion points' (GIP) which are found to be highly significant in the context of compressible flows. If we multiply (5.5) by $\tilde{v}_0^*$ (the complex conjugate of $\tilde{v}_0$) and then subtract from the resulting equation its complex conjugate, the following equation is obtained:

$$\frac{\tilde{v}_0^*}{U_0 - c_0^*}\frac{\mathrm{d}}{\mathrm{d}y}\left\{\frac{(U_0 - c_0)\tilde{v}_{0y} - U_{0y}\tilde{v}_0}{\chi}\right\} = \frac{\tilde{v}_0}{U_0 - c_0}\frac{\mathrm{d}}{\mathrm{d}y}\left\{\frac{(U_0 - c_0^*)\tilde{v}_{0y}^* - U_{0y}\tilde{v}_0^*}{\chi^*}\right\}, \tag{5.6}$$

where

$$\chi = T_0 - M_\infty^2(U_0 - c_0)^2, \tag{5.7}$$

and a superscript asterisk here denotes a complex conjugate. After some algebra, this may be written

$$\tilde{v}_0^*\frac{\mathrm{d}}{\mathrm{d}y}\left[\frac{\tilde{v}_{0y}}{\chi}\right] - \tilde{v}_0\frac{\mathrm{d}}{\mathrm{d}y}\left[\frac{\tilde{v}_{0y}^*}{\chi^*}\right] = \tilde{v}_0\tilde{v}_0^*\left\{\frac{1}{U_0 - c_0}\frac{\mathrm{d}}{\mathrm{d}y}\left[\frac{U_{0y}}{\chi}\right] - \frac{1}{U_0 - c_0^*}\frac{\mathrm{d}}{\mathrm{d}y}\left[\frac{U_{0y}}{\chi^*}\right]\right\}. \tag{5.8}$$

Writing
$$c_0 = \mathrm{Re}\{c_0\} + \mathrm{i}\,\mathrm{Im}\{c_0\} \tag{5.9}$$
then the neutral state corresponds to $\mathrm{Im}\{c_0\} \to 0$. In this limit, (5.8) may be written
$$\frac{\mathrm{d}}{\mathrm{d}y}\left[\frac{\tilde{v}_0^* \tilde{v}_{0y} - \tilde{v}_0 \tilde{v}_{0y}^*}{\chi}\right] = \frac{2\mathrm{i}|\tilde{v}_0|^2 \,\mathrm{Im}\{c_0\}}{|U_0 - c_0|^2} \frac{\mathrm{d}}{\mathrm{d}y}\left[\frac{U_{0y}}{T_0}\right]. \tag{5.10}$$
Using arguments similar to those of Lees & Lin (1946) and Duck (1990), then: (i) as $\mathrm{Im}\{c_0\} \to 0$, the right-hand side of (5.10) is zero except possibly at y_i (where $U_0(y_i) = \mathrm{Re}\{c_0\}$); (ii) the left-hand side of (5.10) must be zero at both $y = 0$ and $y = 1$; while (iii) the right-hand side is clearly non-zero unless
$$\frac{\mathrm{d}}{\mathrm{d}y}\left[\frac{U_{0y}}{T_0}\right]_{y=y_i} = 0. \tag{5.11}$$
Thus, in order to avoid an inconsistency, we must have (5.11).

Most importantly, there does exist a difference between the present (bounded) flow configuration, and that of unbounded flows, in that in the present situation, (5.11) is neccssary if
$$0 < \mathrm{Re}\{c_0\} < 1, \tag{5.12}$$
i.e. a critical layer must exist inside the flow, while in the case of unbounded flows condition (5.11) only holds if the wave speed is 'subsonic', i.e. $1 - 1/M_\infty < \mathrm{Re}\{c_0\} < 1 + 1/M_\infty$. This is because (5.11) is a direct consequence of the zero velocity perturbations at the domain boundaries. In this respect, there is absolutely no distinction made here between supersonic and subsonic modes; thus in a bounded flow, any neutral inviscid mode satisfying (5.12) must be associated with a GIP. Indeed, this point is discernible from the results of Lees & Lin (1946) although it does not appear to have been explicitly pointed out before, at least in the context of internal flows. The above says nothing about neutral inviscid modes outside the range of (5.12). It is also worth noting that authors who implement Dirichlet boundary conditions (in place of radiation boundary conditions) on the disturbance terms in truncated infinite domains may well experience difficulties in computing non-inflexional supersonic modes, since the arguments above suggest that a GIP is necessary for supersonic disturbances, a condition which is clearly erroneous in the unbounded case.

Utilizing (3.5) and (3.9) in (5.11) yields,
$$\left\{\frac{T_{0y}\tau}{\mu_0^2 T_0^2}[\mu_{0T} T_0 + \mu_0]\right\}_{y=y_i} = 0. \tag{5.13}$$
If the term inside the square brackets is zero, then by Sutherland's law (2.9), we must have
$$[3T_0 + 5C]_{y=y_i} = 0, \tag{5.14}$$
which is clearly inadmissible. Consequently, the only way that a GIP will occur is if the mean temperature profile has a local extremum. If we invoke Sutherland's law and (3.9), then we either require
$$U_{0y}(y_i) = 0, \tag{5.15}$$
which is clearly not possible on account of (3.5), or
$$U_0(y_i) = \frac{(1-r)\,T_r}{2[T_r - 1]}. \tag{5.16}$$

Since $T_r > 1$, and the flow is unidirectional, then this condition cannot be satisfied unless

$$0 < U_0(y_i) < 1, \tag{5.17}$$

which implies

$$\frac{1-\frac{1}{2}(\gamma-1)\sigma M_\infty^2}{1+\frac{1}{2}(\gamma-1)\sigma M_\infty^2} < r < 1 \tag{5.18}$$

(implying that the lower wall must be cooled below adiabatic conditions).

6. Inviscid disturbance results

The eigenvalue problem posed in (5.1)–(5.4) was solved using a Runge–Kutta scheme, with Newton iteration being used to update the complex wave speed c_0 so that all boundary conditions were satisfied.

In a number of computations (specifically those for which $0 \leqslant \mathrm{Re}\{c_0\} \leqslant 1$), it was found necessary to deform the integration contour into the complex y-plane (in particular below the real y-axis), in a manner described by Lees & Lin (1946). This was undertaken in two independent ways. The first, as suggested by Mack (1965*b*), involves obtaining the mean flow profile $(U_0(y), T_0(y))$ along the real y-axis, and then using Taylor series expansions to obtain the mean flow profile off the real y-axis; this detour is made close to where $U_0(y) = c_0$. The second approach (which was generally used in preference) obtains the mean flow solution itself in the complex y-plane, thereby eliminating the errors associated with truncation of the Taylor series. Specifically, the mean flow was obtained for $0 \leqslant y \leqslant y_1$ (i.e. on the real y-axis), $y_1 < y \leqslant y_1 - \mathrm{i}y_2$, $y_1 - \mathrm{i}y_2 < y \leqslant y_3 - \mathrm{i}y_2$, $y_3 - \mathrm{i}y_2 < y \leqslant y_3$ and thereafter back along the real axis $y_3 < y \leqslant 1$. y_1, y_2, y_3 were all taken to be real and positive and were chosen to avoid the computation proceeding too close to the critical layer. Comparison of results using the two approaches proved a useful check of the accuracy of our results. A further check on our results was that in addition to solving (5.1), (5.2) we also solved the adjoint system (see (7.20), (7.21) below), and also (5.5).

The first results we present are for the case $M_\infty = 2$ and adiabatic lower-wall boundary conditions. Results for $\mathrm{Re}\{c_0\}$ are shown in figure 8. The results display a number of interesting features. There appear to be many modes, which, however, can be divided into two distinct families, the first corresponding to $\mathrm{Re}\{c_0\} > 1$ as $\alpha \to 0$. All these modes, with the exception of one (mode I) have $\mathrm{Re}\{c_0\} \to \infty$ as $\alpha \to 0$; we refer to these as the upper family. These modes all suffer a monotonic decrease in $\mathrm{Re}\{c_0\}$ as α increases, and the results suggest that some finite value is approached in the limit $\alpha \to \infty$. The second family is defined by $\mathrm{Re}\{c_0\} < 0$ as $\alpha \to 0$, and the $\mathrm{Re}\{c_0\}$ all increase monotonically with an increase in α, and eventually become positive. We refer to these modes as the lower family of solutions. Again, all except the first of these modes (mode II) appear to be unbounded as $\alpha \to 0$.

A further, important feature is that in all cases for which $\mathrm{Re}\{c_0\} > 1$ or $\mathrm{Re}\{c_0\} < 0$, all these modes are neutrally stable to within machine accuracy, i.e. $\mathrm{Im}\{c_0\} = 0$. However, since there can be no GIP point for the mean flow under consideration, then there can be no neutral modes with $0 < c_0 < 1$. Indeed, it is found that in the case of the upper family of solutions, once $\mathrm{Re}\{c_0\} < 1$ these modes become *stable* according to our inviscid calculations, while in the case of the lower family of solutions, once $\mathrm{Re}\{c_0\} > 0$ these modes become *unstable* according to our inviscid calculations; the location at which $\mathrm{Re}\{c_0\}$ either drops below 1 or rises above 0 is marked on figure 8 by a circle. The distribution of $\mathrm{Im}\{c_0\}$ for mode I is shown in figure 9(*a*) (other upper-

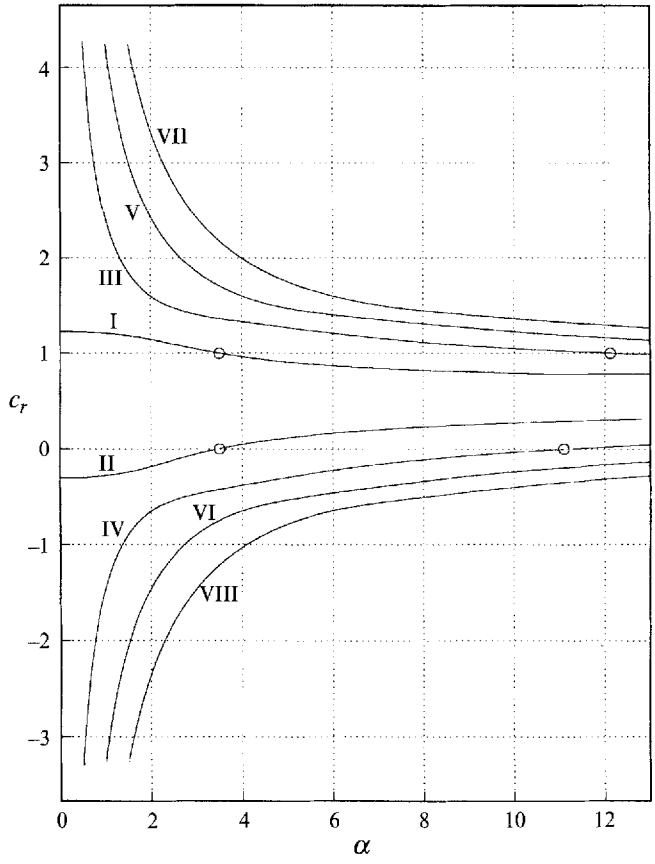

FIGURE 8. $Re\{c_0\}$ as a function of α for $M_\infty = 2$, adiabatic lower wall.

family modes also have negative values of $\mathrm{Im}\{c_0\}$, but many orders of magnitude smaller). The distribution of $\mathrm{Im}\{c_0\}$ for mode II is shown in figure 9(*b*) (other modes of the lower family have considerably smaller values of $\mathrm{Im}\{c_0\}$, although these are also positive). Note that Tam & Hu (1989*b*) studied mixing layers in a confined region, and showed the existence of four families of modes, two of them neutral, and two of them unstable. The unstable families depended on the existence of a small region of subsonic flow confined between two regions of relatively supersonic flow.

Next we go on to consider the aforementioned trends as $\alpha \to 0$ suggested by our numerical results. The existence and behaviour of modes I and II as $\alpha \to 0$ is easy to confirm. If we set $\alpha = 0$ in (5.5), and integrate once, we obtain

$$(U_0 - c_0)\tilde{v}_{0y} - U_{0y}\tilde{v}_0 = K[T_0 - M_\infty^2(U_0 - c_0)^2], \tag{6.1}$$

where K is an arbitrary constant. This equation may be integrated once more to yield

$$\tilde{v}_0 = K(U_0 - c_0)\int_0^y \frac{[T_0 - M_\infty^2(U_0 - c_0)^2]}{(U_0 - c_0)^2}\,\mathrm{d}y. \tag{6.2}$$

If this is to satisfy the boundary condition on $y = 1$ (the boundary condition on $y = 0$ is already satisfied by (6.2)), the integrand of (6.2) must possess at least one zero, which implies the presence of at least one solid line. Thus, c_0 must satisfy

$$\int_0^1 \frac{T_0}{(U_0 - c_0)^2}\,\mathrm{d}y = M_\infty^2, \tag{6.3}$$

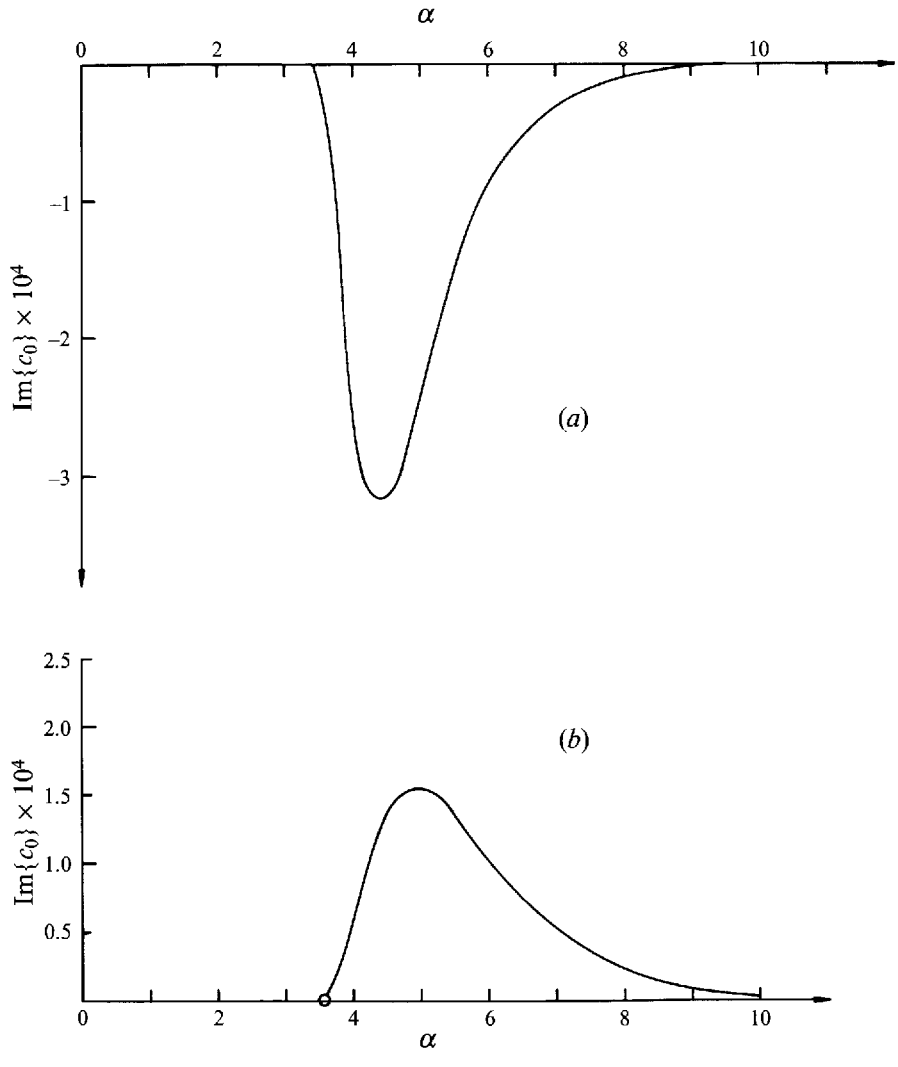

FIGURE 9. $\mathrm{Im}\{c_0\}$ as a function of α for $M_\infty = 2$, adiabatic lower wall: (*a*) mode I; (*b*) mode II.

a result which is similar to that found in certain classes of incompressible flow (e.g. Miles 1961). Solving (6.3) c_0 (for given $U_0(y)$, $T_0(y)$, and M_∞) confirmed the numerical results as $\alpha \to 0$. Indeed, if we take a model problem, i.e.

$$U_0(y) = y, \quad T_0(y) = 1 \tag{6.4}$$

then the solutions of (6.3) are

$$c_0 = \tfrac{1}{2}(1 \pm [1 + 4/M_\infty^2]^{\frac{1}{2}}). \tag{6.5}$$

These modes will be discussed further in §7.

The behaviour of modes III and higher as $\alpha \to 0$ is different, but nonetheless, straightforward to confirm. In these cases we have $c_0 \to \infty$ as $\alpha \to 0$, and a balancing of terms in (5.5) in this limit demands

$$c_0 = \alpha^{-1} c_{00} + O(1), \tag{6.6}$$

$$\tilde{v}_0 = \tilde{v}_{00} + O(\alpha). \tag{6.7}$$

The equation for $\tilde{v}_{00}$ is then

$$\tilde{v}_{0yy}+\frac{c_{00}^2 M_\infty^2 \tilde{v}_{00}}{T_0}=0. \tag{6.8}$$

If, to make further progress analytically, we assume $|c_{00}| \gg 1$, implying that we are focusing attention on the higher nodes (alternatively we could assume the model problem, with $T_0 = 1$), then the WKB solution is

$$v_{00} = AT_0^{\frac{1}{4}}\left\{\exp\left[\mathrm{i}c_{00}M_\infty\int_0^y T_0^{-\frac{1}{2}}\mathrm{d}y\right]-\exp\left[-\mathrm{i}c_{00}M_\infty\int_0^y T_0^{-\frac{1}{2}}\mathrm{d}y\right]\right\}, \tag{6.9}$$

where A is a constant. Here the boundary condition on $y = 0$ has been applied, while the other boundary condition on $y = 1$ demands

$$c_{00} = \frac{n\pi}{M_\infty\int_0^1 T_0^{-\frac{1}{2}}\mathrm{d}y}, \tag{6.10}$$

where n is any (large) positive or negative integer. This expression clearly illustrates the multiplicity of modes.

We can now explain intuitively why the upper family of modes (I, III, V, ...) is stable, while the other family of modes (II, IV, ...) have regions of instability by contrasting with what is known in the boundary layer. The analysis hinges on the size of the relative Mach number at the two walls. Starting from the definition of relative Mach number

$$M_r = \frac{U_0(y)-c}{[T_0(y)]^{\frac{1}{2}}}M_\infty$$

it is easy to show that the top boundary is relatively supersonic $|M_r| > 1$ when $c > 1+1/M_\infty$, or $c < 1-1/M_\infty$. On the other hand, the bottom boundary (assumed adiabatic with a wall temperature given by (3.7)), is relatively supersonic when the phase velocity approximately satisfies $c < -T_w^{\frac{1}{2}}/M_\infty$ or $c > T_w^{\frac{1}{2}}/M_\infty$. Immediately, we see that as M_∞ increases, the range of c_0 over which the top boundary is subsonic decreases, while the range of c_0 over which the bottom boundary is subsonic tends to a finite limit. Considering first the even-numbered family of modes when $\mathrm{Re}\{c_0\} > 0$, we find that the bottom wall is relatively subsonic, while the top wall is relatively supersonic. Thus, the situation can be compared to that found in an unconfined flow over a flat plate when there is an imbedded supersonic flow between the wall and the relative sonic line. Both for the unconfined flows, and the Couette flow, the second mode is unstable. Consider now the odd-numbered family of modes for $\mathrm{Re}\{c_0\} < 1$ as M_∞ increases. Both the top and bottom boundaries are relatively supersonic, separated by a region of subsonic flow. This situation is reminiscent of that described in Tam & Hu (1989*b*). They found two families of unstable modes when a vortex sheet was separated by two regions of uniform flow, both relatively supersonic. When the thickness of the vortex sheet became finite and was increased, the magnitude of the growth rate decreased, but remained positive. However, there was always a region of uniform flow on either side of the shear layer which could sustain sinusoidal waves. If the width of the shear layer in Tam & Hu (1989*b*) were to extend across the whole domain, the instabilities would probably disappear, which would be consistent with our results.

The second set of results we show is for the higher Mach number case $M_\infty = 5$, with the adiabatic boundary conditions on the lower wall retained. Figure 10(*a*) shows a

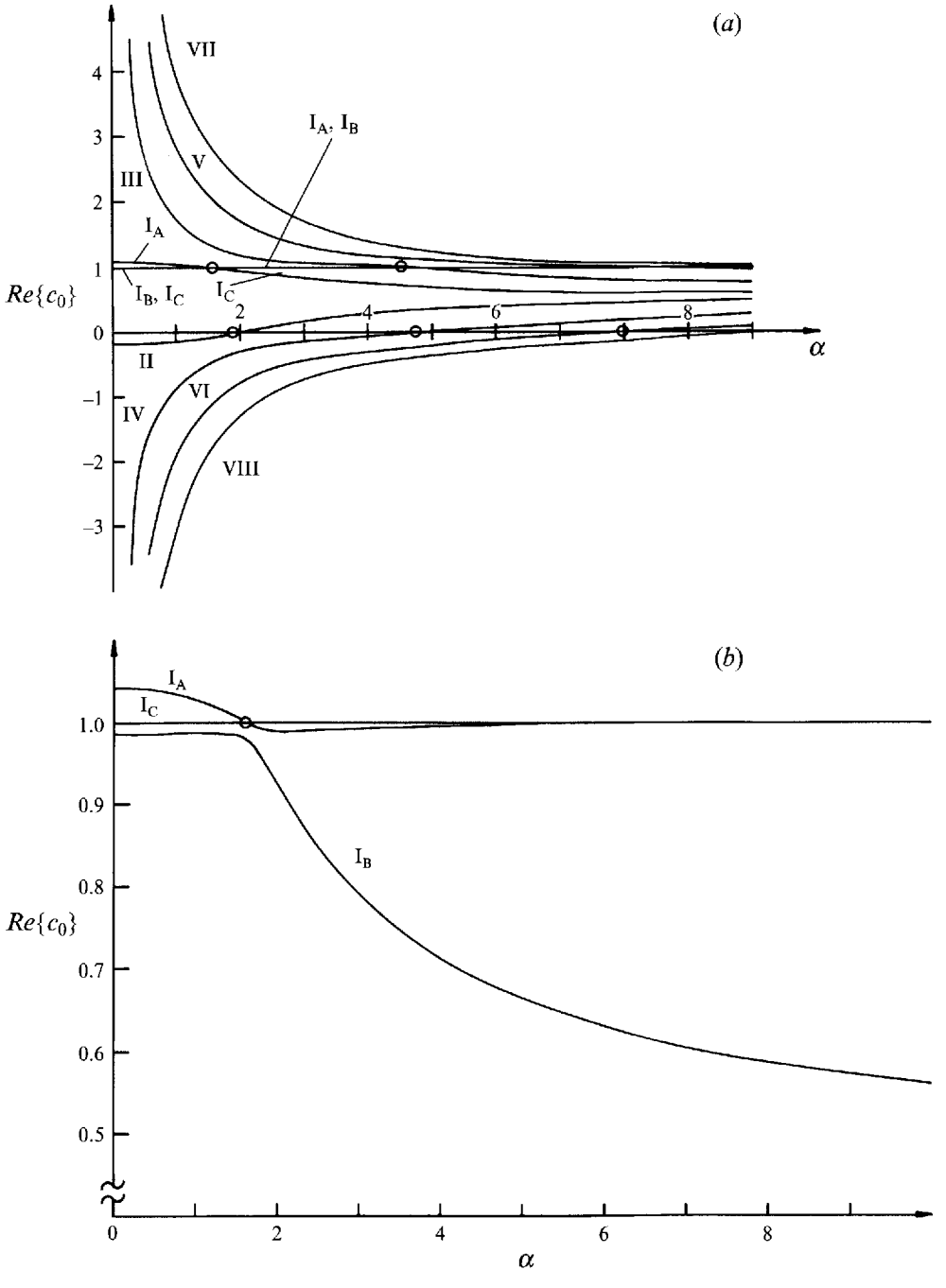

FIGURE 10. $\mathrm{Re}\{c_0\}$ as a function of α for $M_\infty = 5$, adiabatic lower wall: (*a*) mode II; (*b*) modes I_A, I_B, I_C.

number of results for $\mathrm{Re}\{c_0\}$. Although these seem much the same as the corresponding distributions for $M_\infty = 2$ there are some differences, in particular with mode I_A, as defined in figure 10(*a*), which initially corresponds to mode I in figure 9(*a*). However, unlike the corresponding results for $M_\infty = 2$, it turns out that there exist other (stable) modes in the vicinity of mode I_A. Some of these modes are shown in figure 10(*b*) (on

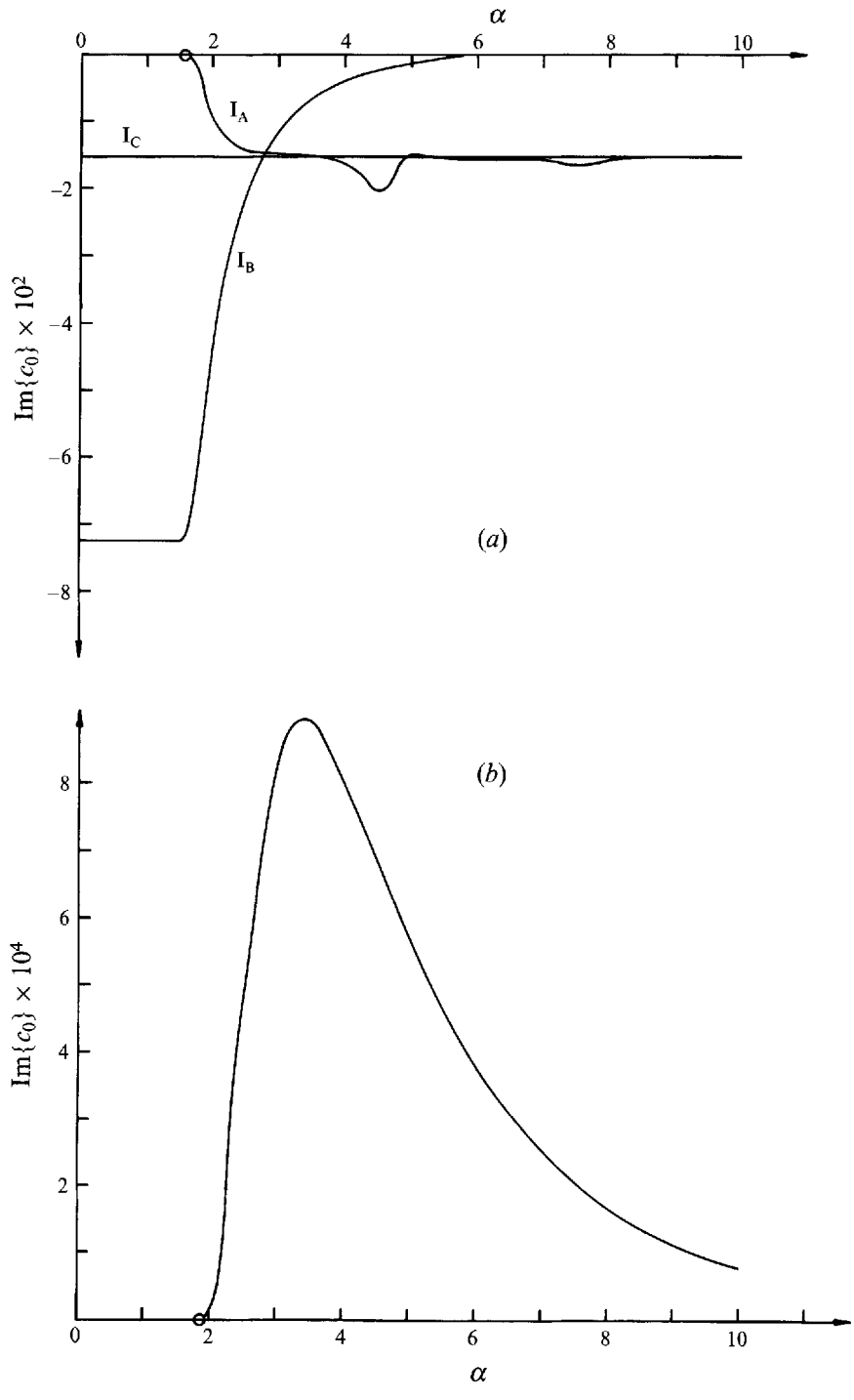

FIGURE 11. $\mathrm{Im}\{c_0\}$ as a function of α for $M_\infty = 5$, adiabatic lower wall: (*a*) modes I_A, I_B, I_C; (*b*) mode II.

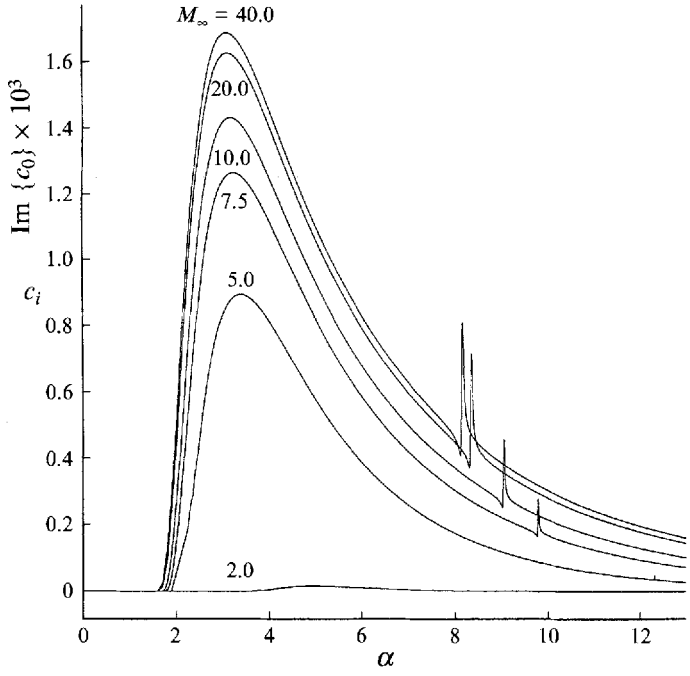

FIGURE 12. Im$\{c_0\}$ as a function of α, increasing M_∞, adiabatic lower wall, mode II.

a magnified scale) and are denoted by $\mathrm{I_B}$ and $\mathrm{I_C}$. These modes were difficult to generate numerically in regions of α where Re$\{c_0\}$ was very close to unity and where the decay rates were quite small; however, the existence of these modes was confirmed using the three different formulations of the inviscid stability problem described above, together with the condition (6.3). Indeed, it is quite likely that other such modes exist, although the present investigation failed to yield any. However, it turns out that these modes are all stable, as shown in figure 11(*a*). Note that modes $\mathrm{I_A}$ and $\mathrm{I_C}$ have, in places, values of c_0 exceedingly close to each other, but nonetheless distinct; this compounded the difficulty associated with these modes.

Modes II and higher, on the other hand, did exhibit the same qualitative behaviour as the corresponding $M_\infty = 2$ results. In particular, mode II becomes unstable at $\alpha \approx 1.85$, with the distribution of Im$\{c_0\}$ shown in figure 11(*b*). Other higher modes of this lower family are also unstable, but with substantially smaller growth rates.

We next consider the effect of increasing the Mach number M_∞ on the important (unstable) mode II, for the adiabatic lower-wall case. This is shown in figure 12. It is very clear that as M_∞ increases, Im$\{c_0\}$ approaches a finite limit. This is interesting in so far as in many other examples, such as boundary layers and shear layers, an increase in Mach number results in a decrease in the growth rate. However, there is a very simple explanation for this trend in our case. As $M_\infty \to \infty$, we expect that (generally) $T_0 \to M_\infty^2 \hat{T}_0(y)$, $\hat{T}_0 = O(1)$, whilst all other quantities remain bounded in this limit. Thus, (5.5) reduces to

$$\frac{\mathrm{d}}{\mathrm{d}y}\left\{\frac{(\hat{U}_0 - c_0)\tilde{v}_{0y} - \hat{U}_{0y}\tilde{v}_0}{\hat{T}_0 - (\hat{U}_0 - c_0)^2}\right\} = \frac{\alpha^2(\hat{U}_0 - c_0)}{\hat{T}_0}\tilde{v}_0, \tag{6.11}$$

and numerical solutions of this system by T. James (1993, private communication) confirm the trends observed in our numerical results.

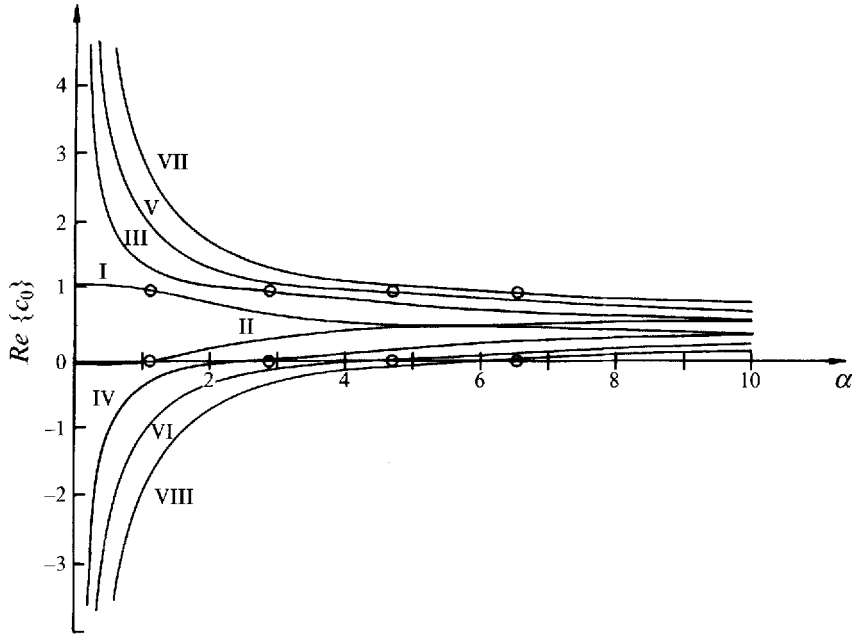

FIGURE 13. $\mathrm{Re}\{c_0\}$ as a function of α for $M_\infty = 5$, $T(0) = 1$.

The existence of the 'kinks' that are observed in the distributions shown in figure 12 are a surprise indeed. Careful numerical checks were performed, including grid resolution, and changes in the indentation of integration contours in complex space. All the results indicate that these 'kinks' are real, although they are probably not physically significant.

The final set of results in this section relates to the case $M_\infty = 5$, as previously, but with the (cooled-wall) boundary condition $T_0(0) = 1$. It is worth noting that, even in this case, the uniform temperature together with a linear velocity profile is still not a proper solution of the governing equations, except in the very special limit as $\gamma \to 1$. Nonetheless, the proper solution does have some important properties, namely that

$$T_0(y) = T_0(1-y), \tag{6.12}$$

together with

$$U_0(y) = 1 - U_0(1-y). \tag{6.13}$$

As a consequence of these symmetries, the mean flow has a single GIP at $y = \frac{1}{2}$ (with $U_0(\frac{1}{2}) = \frac{1}{2}$). These properties turn out to have interesting implications for the inviscid stability of the profile.

Figure 13 shows the variations of $\mathrm{Re}\{c_0\}$ for the first eight modes. As in the previous cases, there again exist two distinct families, with all except two of the modes having the property $|\mathrm{Re}\{c_0\}| \to \infty$ as $\alpha \to 0$. Furthermore, all modes are neutrally stable if $\mathrm{Re}\{c_0\} < 0$ or $\mathrm{Re}\{c_0\} > 1$. Significantly, owing to the aforementioned asymmetries about $y = \frac{1}{2}$, the behaviour of $\mathrm{Re}\{c_0\}$ for the upper family of modes is merely the mirror image of the corresponding lower family member about $\mathrm{Re}\{c_0\} = \frac{1}{2}$. These symmetries also yield the result that $\mathrm{Im}\{c_0\}$ is precisely the same for corresponding modes at the same wavenumber. Figure 14(*a*) shows the distribution of $\mathrm{Im}\{c_0\}$ for modes I and II. These modes are initially neutrally stable, then as $\mathrm{Re}\{c_0\}$ drops below unity/rises above zero both modes become stable. As α increases still further, both modes have $\mathrm{Re}\{c_0\} \to \frac{1}{2}$ which is reached at $\alpha \approx 0.5$. $\mathrm{Im}\{c_0\}$ then becomes positive, implying unstable

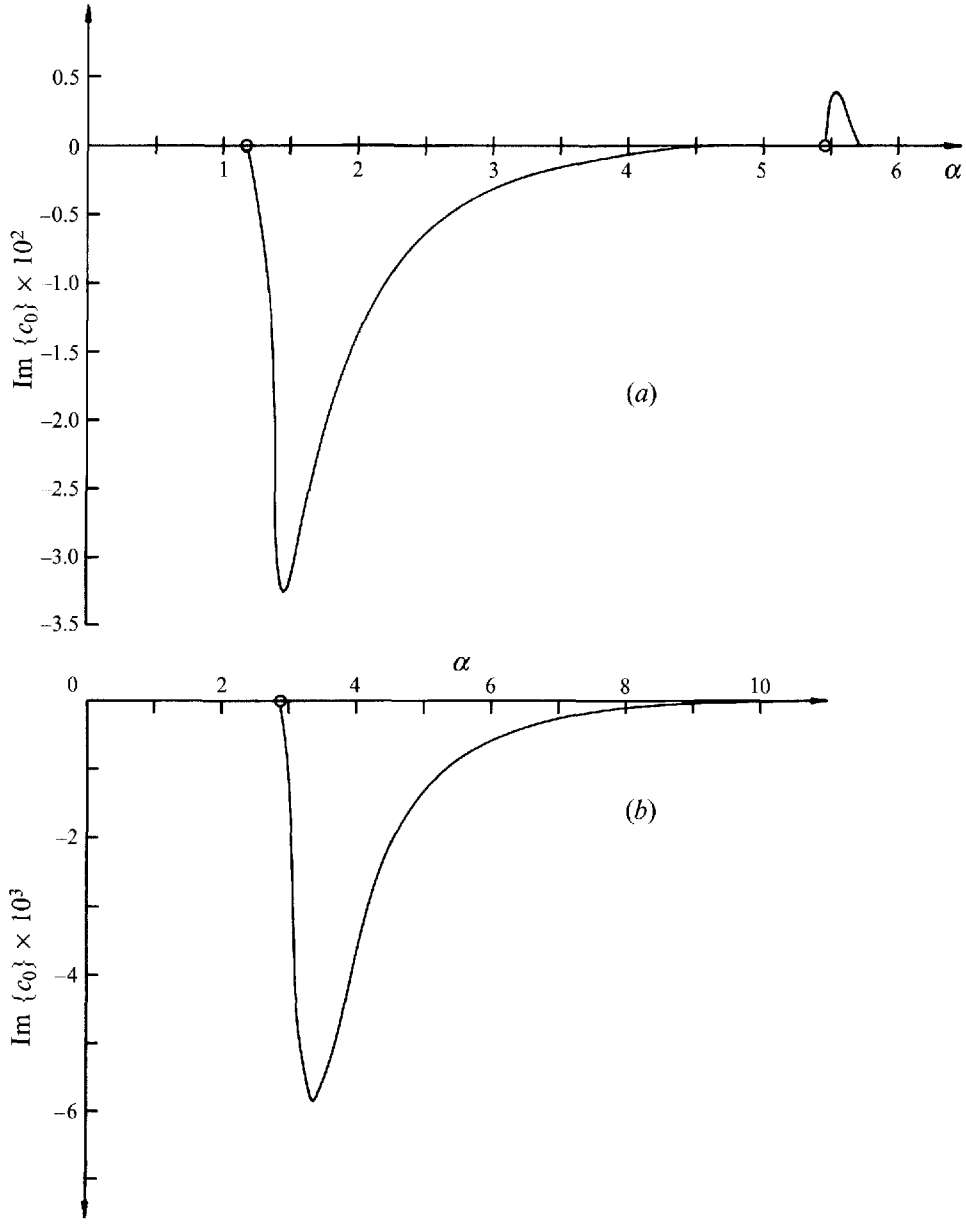

FIGURE 14. $\mathrm{Im}\{c_0\}$ as a function of α for $M_\infty = 5$, $T(0) = 1$: (*a*) modes I and II; (*b*) modes III and IV.

modes. This is entirely consistent with our GIP arguments, which predict neutral modes having $c_0 = \frac{1}{2}$. Thereafter, $\mathrm{Re}\{c_0\}$ for mode I increases, and decreases for mode II.

Figure 14(*b*) shows the distribution of $\mathrm{Im}\{c_0\}$ for modes III and IV (which have identical values of $\mathrm{Im}\{c_0\}$), which over the range shown are seen to be stable. It is possible that regions of instability exist for higher α, although the computations become increasingly difficult as $\alpha \to \infty$.

In the following section, we go on to consider regions where viscous effects are likely to become important, particularly in determining the stability properties of the flow.

7. The viscous correction

The results described in the previous sections show that there is a family of solutions of (5.1)–(5.4) comprising neutrally stable modes over a wide range of α, which have either $c_0 > 1$, or $c_0 < 0$, and hence have no critical layer. The question then arises as to the effect of viscosity on these modes – whether it plays a stabilizing or destabilizing role in this problem. We investigate this question next.

The viscous correction to the problem arises due to the thin layers that occur as a result of the violation of the no-slip condition (and also the temperature condition) on the walls $y = 0$ and $y = 1$. These conditions are

$$\tilde{u} = \tilde{v} = 0 \quad \text{on} \quad y = 0 \quad \text{and} \quad y = 1, \tag{7.1}$$

$\tilde{T} = 0$ on $y = 1$, while on $y = 0$,

$$\frac{\partial \tilde{T}}{\partial y} = 0 \tag{7.2}$$

if the wall is insulated, and

$$\tilde{T} = 0 \tag{7.3}$$

if it is heated or cooled.

Now from (4.4) and (4.6) we see that on $y = 0$ we have

$$\tilde{u}_0 = \frac{T_0(0)\tilde{p}_0(0)}{\gamma M_\infty^2 c_0} \tag{7.4}$$

and

$$\tilde{T}_0 = \left(\frac{\gamma - 1}{\gamma}\right) T_0(0)\tilde{p}(0), \tag{7.5}$$

while on $y = 1$ we have

$$\tilde{u}_0 = \frac{T_0(1)\tilde{p}_0(1)}{\gamma M_\infty^2 (c_0 - 1)} \tag{7.6}$$

and

$$\tilde{T}_0 = \left(\frac{\gamma - 1}{\gamma}\right) T_0(1)\tilde{p}_0(1). \tag{7.7}$$

Thus generally these expressions fail to satisfy the appropriate wall conditions described above.

In order to remedy this, we require a (Stokes-like) layer of thickness $O(Re^{-\frac{1}{2}})$ on both walls. Considering first the layer on $y = 0$, defining

$$Y = y\, Re^{\frac{1}{2}} = O(1), \tag{7.8}$$

together with

$$\left.\begin{aligned} &\tilde{u} = \tilde{U}(Y) + O(Re^{-\frac{1}{2}}), \quad \tilde{v} = Re^{-\frac{1}{2}}\tilde{V}(Y) + O(Re^{-1}), \\ &\tilde{T} = \tilde{\tilde{T}}(Y) + O(Re^{-\frac{1}{2}}), \quad \tilde{p} = \tilde{P}(Y) + O(Re^{-\frac{1}{2}}), \end{aligned}\right\} \tag{7.9}$$

then taking $O(1)$ terms in (4.3)–(4.7), we find

$$\tilde{U} = \frac{\tilde{p}_L T_0(0)}{\gamma M_\infty^2 c_0}\left\{1 - \exp\left[-\left(\frac{-i\alpha c_0}{T_0(0)\mu_L}\right)^{\frac{1}{2}} Y\right]\right\}, \tag{7.10}$$

where $\mu_L = \mu_0(0)$, $\tilde{p} = \tilde{p}_L = \tilde{p}_0(0)$.

The corresponding layer on the upper wall is quite similar. Defining the lengthscale

$$\hat{Y} = (y - 1)\, Re^{\frac{1}{2}},$$

together with (7.9), then the results for $\hat{Y} = O(1)$ may be simply inferred from those for $Y = O(1)$ by: (i) replacing Y by $-\hat{Y}$; (ii) replacing $\tilde{p}_L$ by $\tilde{p}_U = \tilde{p}(1)$; (iii) replacing c_0 by $c_0 - 1$; and (iv) replacing μ_L and $T_0(0)$ by unity.

We require the behaviour of $\tilde{V}$ as $Y \to \infty$ and $\hat{Y} \to -\infty$, respectively. Using the above, we find

$$\tilde{V} \to Y\left\{ic_0\tilde{p}_L - ic_0 p_L\left(\frac{\gamma-1}{\gamma}\right) - i\frac{\tilde{p}_L}{\gamma M_\infty^2 c_0}\right\}$$

$$+\frac{ic_0\tilde{p}_L b\left(\frac{\gamma-1}{\gamma}\right)}{\left[\frac{-i\alpha c_0\sigma}{T_0(0)\mu_L}\right]^{\frac{1}{2}}} + \frac{i\tilde{p}_L T_0(0)}{\gamma M_\infty^2 c_0\left[\frac{-i\alpha c_0}{T_0(0)\mu_L}\right]^{\frac{1}{2}}} \tag{7.11}$$

$$\to \tilde{v}_{0L} Y + \tilde{v}_{1L} \quad \text{as} \quad Y \to \infty, \tag{7.12}$$

and

$$\tilde{V} \to \hat{Y}\left\{i(c_0-1)\tilde{p}_U - \frac{i(c_0-1)\tilde{p}_U\left(\frac{\gamma-1}{\gamma}\right)}{[-i\alpha(c_0-1)\sigma]^{\frac{1}{2}}} - \frac{i\tilde{p}_U}{\gamma M_\infty^2(c_0-1)[-i\alpha(c_0-1)]^{\frac{1}{2}}}\right\}$$

$$-\frac{i(c_0-1)\tilde{p}_U\left(\frac{\gamma-1}{\gamma}\right)}{[-i\alpha(c_0-1)\sigma]^{\frac{1}{2}}} - \frac{i\tilde{p}_U}{\gamma M_\infty^2(c_0-1)[-i\alpha(c_0-1)]^{\frac{1}{2}}} \tag{7.13}$$

$$\to \tilde{v}_{0U}\hat{Y} + \tilde{v}_{1U} \quad \text{as} \quad \hat{Y} \to -\infty, \tag{7.14}$$

where $b = 0$ in the case of an insulated wall, while $b = 1$ for a cooled/heated wall.

We now seek the leading-order viscous correction term to (5.1), (5.2) for $y = O(1)$, using the expansions (4.14). The variables $\tilde{v}_1$ and $\tilde{p}_1$ turn out to be determined by an inhomogeneous form of (5.1) and (5.2), namely

$$\tilde{v}_{1y} - \frac{U_{0y}\tilde{v}_1}{U_0 - c_0} - \frac{i\tilde{p}_1}{U_0 - c_0}\left[\frac{T_0 - M_\infty^2(U_0-c_0)^2}{\gamma M_\infty^2}\right] = c_1 R_1, \tag{7.15}$$

$$\tilde{p}_{1y} + \frac{i\alpha^2\gamma M_\infty^2}{T_0}(U_0 - c_0)\tilde{v}_1 = c_1 R_2, \tag{7.16}$$

where

$$R_1 = \frac{U_{0y}\tilde{v}_0}{(U_0-c_0)^2} + \frac{i\tilde{p}_0 T_0}{\gamma M_\infty^2(U_0-c_0)^2} + \frac{i\tilde{p}_0}{\gamma}, \tag{7.17}$$

$$R_2 = \frac{i\gamma M_\infty^2\alpha^2\tilde{v}_0}{T_0}. \tag{7.18}$$

The boundary conditions on this system are also inhomogeneous, namely

$$\tilde{v}_1(0) = \tilde{v}_{1L}, \quad \tilde{v}_1(1) = \tilde{v}_{1U} \tag{7.19}$$

(the boundary conditions for $\tilde{p}_{1y}$ may be obtained from (7.16), although this is not necessary for the following), where $\tilde{v}_{1L}$ and $\tilde{v}_{1U}$ are defined by (7.12) and (7.14) respectively.

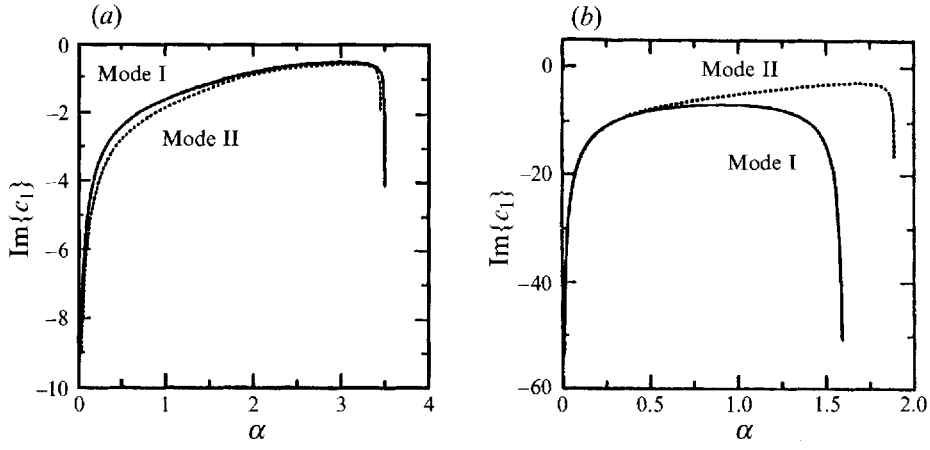

FIGURE 15. Im$\{c_1\}$ as a function of α for adiabatic lower wall, modes I and II: (*a*) $M_\infty = 2$; (*b*) $M_\infty = 5$.

To obtain c_1, we use the condition of solvability of the system (7.15)–(7.19). For this we require the adjoint to the system; if we denote v^+ and p^+ as the adjoint functions, then these are to be determined by

$$v_y^+ + \frac{U_{0y} v^+}{U_0 - c_0} + \frac{\mathrm{i}\alpha^2 (U_0 - c_0)\gamma M_\infty^2}{T_0} p^+ = 0, \tag{7.20}$$

$$p_y^+ - \frac{\mathrm{i}v^+}{U_0 - c_0}\left[\frac{T_0 - M_\infty^2 (U_0 - c_0)^2}{\gamma M_\infty^2}\right] = 0. \tag{7.21}$$

The boundary conditions to be applied to this system are that

$$p^+(0) = p^+(1) = 0. \tag{7.22}$$

c_1 is then given by

$$c_1 = \frac{v^+(1)\tilde{v}_{1U} - v^+(0)\tilde{v}_{1L}}{\int_0^1 [R_1 \bar{v}^+ + R_2 \bar{p}^+]\,\mathrm{d}y}, \tag{7.23}$$

where $\bar{v}^+$ and $\bar{p}^+$ are the complex conjugates of v^+ and p^+ respectively.

Given the nature of the solution for v^+, p^+, $\tilde{v}_{1U}$, $\tilde{v}_{1L}$, $\bar{R}$, and R_2 when c_0 is real, it is easy to show that we must have

$$c_1 = \mathrm{Im}\{c_1\}(\pm 1 + \mathrm{i}), \tag{7.24}$$

where the positive sign is taken for $c_0 > 0$, the negative sign is taken for $c_0 < 0$; note that $\mathrm{Im}\{c_1\} > 0$ for instability. However, in all the computations we performed, without exception, we found $\mathrm{Im}\{c_1\} < 0$. Results for $\mathrm{Im}\{c_1\}$ for the adiabatic case with $M_\infty = 2$ (modes I and II) are shown in figure 15(*a*). The distribution becomes unbounded as $\alpha \to 0$, and also as $\alpha \to \alpha_0$, the point at which $c_0 \to 1$ or 0; these distributions are typical of all modes. Figure 15(*b*) shows the corresponding distributions for the adiabatic case with $M_\infty = 5$, and exhibit, qualitatively, the same behaviour. (The corresponding computation for $M_\infty = 5$, $T_0(0) = 1$ was also carried out, and yielded qualitatively the same picture.) We shall defer discussion of the limit $\alpha \to \alpha_0$ until the following section, but let us now consider the limit as $\alpha \to 0$ of modes

I and II, from which it appears that our expansions cease to be uniformly valid. This is most clearly seen by the apparently singular behaviour of the viscous correction to the complex wave speed as $\alpha \to 0$, together with the $O(\alpha^{-\frac{1}{2}})$ growth of the wall-layer thickness in this limit (see (7.10) for example). Thus when $\alpha = O(Re^{-1})$ the wall layers will fill the entire channel, and the disturbances become purely viscous in nature.

Specifically, if we write

$$\alpha = Re^{-1}\bar{\alpha}, \tag{7.25}$$

then the governing equations (4.3)–(4.6) reduce to

$$-\mathrm{i}c\tilde{\rho} + \mathrm{i}\rho_0\tilde{u} + \rho_0\tilde{v} + \mathrm{i}U_0\tilde{\rho} + \tilde{v}\rho_{0y} = 0, \tag{7.26}$$

$$\bar{\alpha}\rho_0[-\mathrm{i}c\tilde{u} + \mathrm{i}U_0\tilde{u} + \tilde{v}U_{0y}] + \frac{\mathrm{i}\bar{\alpha}\tilde{p}}{\gamma M_\infty^2} = \mu_0\tilde{u}_{yy} + \mu_{0T}\tilde{T}U_{0y} + \mu_{0T}T_{0y}\tilde{u}_y, \tag{7.27}$$

$$\tilde{p}_y = 0, \tag{7.28}$$

$$\bar{\alpha}\rho_0[-\mathrm{i}c\tilde{T} + \mathrm{i}U_0\tilde{T} + \tilde{v}T_{0y}] - \left(\frac{\gamma-1}{\gamma}\right)[\mathrm{i}\bar{\alpha}U_0 - \mathrm{i}\bar{\alpha}c]\tilde{p}$$

$$= \frac{\mu_0}{\sigma}\tilde{T}_{yy} + \frac{\mu_{0T}}{\sigma}T_{0y}\tilde{T}_y + \frac{\tilde{T}\mu_{0T}}{\sigma}T_{0yy} + \frac{\tilde{T}_y\mu_{0T}}{\sigma} + \tilde{T}\mu_{0TT}T_{0y} + \tilde{T}\mu_{0T}(\gamma-1)M_\infty^2 U_{0y}^2, \tag{7.29}$$

where it has been implicitly assumed that viscosity is a function of temperature only. The problem then reduces to a basically viscous system.

However, for modes III and higher, $c_0 = O(\alpha^{-1})$ as $\alpha \to 0$, and since the Stokes-layer thickness remains $O(R^{-\frac{1}{2}})$, it does not fill the entire channel. Additionally, as $\alpha \to 0$, $\mathrm{Im}\{c_1\} = O(\alpha^{-1})$, and so the expansions (4.14) remain valid.

Returning to figure 7(*b*), we note the generally excellent agreement between the values of $Re^{\frac{1}{2}}\mathrm{Im}\{c\}$ obtained numerically, and $\mathrm{Im}\{c_1\}$ obtained from the above asymptotic theory, for the case $M_\infty = 2$ (mode II). The values of c_r obtained using the two approaches are almost indistinguishable. We do note a deviation between the results as $c_0 \to 0$, caused by the (expected) breakdown in the asymptotic theory in this limit (and as $c_0 \to 1$). This aspect is investigated in the following section.

8. The nature of the solution as $c_0 \to 0$ (or $c_0 \to 1$)

We consider here the nature of the complex wave speed as $c_0 \to 0$ (the results for $c_0 \to 1$ may be simply inferred from those of $c_0 \to 0$). Our previous results indicate that as $c_0 \to 0$, (with $\alpha \to \alpha_0$) then: (i) c_1, the viscous correction to the wave speed becomes unbounded; (ii) the leading-order wave speed c_0 becomes non-neutral as α increases above α_0; and (iii) the thickness of the wall layer increases. Thus the region is likely to be a regime of some interest, on which we now focus our attention.

More specifically, if we write

$$\alpha = \alpha_0 + \epsilon\alpha_1, \tag{8.1}$$

where

$$\epsilon = Re^{-\frac{1}{3}}, \tag{8.2}$$

then we expect

$$c = \epsilon\hat{c}_1 + O(\epsilon^{\frac{3}{2}}). \tag{8.3}$$

The solution in the 'core', i.e. away from the wall layers is then expected to develop in the form

$$\tilde{v} = \hat{v}_0(y) + \epsilon\hat{v}_1(y) + \ldots, \tag{8.4}$$

$$\tilde{p} = \hat{p}_0(y) + \epsilon\hat{p}_1(y) + \ldots. \tag{8.5}$$

The leading-order system is then

$$\hat{v}_{0y} - \frac{U_{0y}\hat{v}_0}{U_0} - \frac{\mathrm{i}\hat{p}_0}{\gamma M_\infty^2 U_0}[T_0 - M_\infty^2 U_0^2] = 0, \tag{8.6}$$

or symbolically

$$\mathscr{L}_1\{\hat{v}_0, \hat{p}_0\} = 0, \tag{8.7}$$

and

$$\frac{\hat{p}_{0y}}{\gamma M_\infty^2} + \mathrm{i}\alpha_0^2 \frac{U_0 \hat{v}_0}{T_0} = 0, \tag{8.8}$$

or symbolically

$$\mathscr{L}_2\{\hat{v}_0, \hat{p}_0\} = 0, \tag{8.9}$$

together with

$$\hat{v}_0(0) = \hat{v}_0(1) = 0. \tag{8.10}$$

Notice that (8.6) and (8.8) imply that $\hat{p}_0 = O(y^3)$ as $y \to 0$; this system effectively determines the value(s) of α_0 for which $c_0 = 0$. Turning to the next-order system, we find

$$\mathscr{L}_1\{\hat{v}_1, \hat{p}_1\} = U_{0y}\frac{\hat{v}_0 \hat{c}_1}{U_0^2} + \frac{\mathrm{i}\hat{p}_0}{\gamma M_\infty^2 U_0^2}\hat{c}_1[T_0 + M_\infty^2 U_0^2] = \hat{c}_1 \hat{R}_1, \tag{8.11}$$

$$\mathscr{L}_2\{\hat{v}_1, \hat{p}_1\} = \frac{\mathrm{i}\alpha_0^2 \hat{c}_1 \hat{v}_0}{T_0} - \frac{2\mathrm{i}\alpha_0 \alpha_1 U_0 \hat{v}_0}{T_0} = \hat{c}_1 \hat{R}_2 + \alpha_1 \hat{R}_3. \tag{8.12}$$

The boundary conditions to be applied to this system are

$$\hat{v}_1(1) = 0, \quad \hat{v}_1(0) = A\hat{p}_1(0), \tag{8.13}$$

where A is to be determined later. Using conditions of solvability, we must have that

$$\hat{c}_1 = \frac{-\hat{v}^+(0) A\hat{p}_1(0) - \alpha_1 \int_0^1 \hat{R}_3 \hat{p}^+ \,\mathrm{d}y}{\int_0^1 [\hat{R}_1 \hat{v}^+ + \hat{R}_2 \hat{p}^+]\,\mathrm{d}y}, \tag{8.14}$$

where $\hat{p}^+(y)$, $\hat{v}^+(y)$ are the adjoint functions to (8.6), (8.8), namely those determined by (7.20), (7.21) with $\alpha = \alpha_0$, $c_0 = 0$.

We now consider the effect of the wall layers. The upper wall layer remains of thickness $O(Re^{-\frac{1}{3}})$ and as such plays no role to this order. The interesting changes are related to the lower wall layer, where now we must have

$$\tilde{Y} = \epsilon^{-1} y = O(1) \tag{8.15}$$

as the crucial scale, wherein to leading order

$$(\tilde{u}, \tilde{v}, \tilde{p}) = (\tilde{U}_0, \epsilon \tilde{V}_0, \epsilon \tilde{P}_0). \tag{8.16}$$

Taking the leading-order terms in the continuity and momentum equations we find

$$\mathrm{i}\tilde{U}_0 + \tilde{V}_{0\tilde{Y}} = 0, \tag{8.17}$$

$$\tilde{P}_{0\tilde{Y}} = 0, \tag{8.18}$$

$$\mathrm{i}\alpha_0[U_0'(0)\,\tilde{Y} - \hat{c}_1]\,\tilde{U}_0 + \alpha_0 U_0'(0)\,\tilde{V}_0 = \tilde{U}_{0\tilde{Y}\tilde{Y}} - \mathrm{i}\alpha_0 \tilde{P}_0, \tag{8.19}$$

with boundary conditions

$$\tilde{U}_0(0) = \tilde{V}_0(0) = 0,$$

and as $\tilde{Y} \to \infty$

$$\tilde{U}_0 \to -\mathrm{i}\hat{v}_{0y}(0), \tag{8.20}$$

where the latter condition arises from a proper matching with the $y = O(1)$ solution. If we now differentiate (8.19) with respect to $\tilde{Y}$, invoke (8.17) and (8.18) we find

$$\tilde{U}_{0\tilde{Y}\tilde{Y}\tilde{Y}} - \mathrm{i}\alpha_0[U_0'(0)\,\tilde{Y} - \hat{c}_1]\,\tilde{U}_{0\tilde{Y}} = 0. \tag{8.21}$$

The solution of this equation (utilizing the boundary condition on $Y = 0$, and also evaluating (8.19) on $\tilde{Y} = 0$), leads to

$$\tilde{U}_0 = \frac{\mathrm{i}\alpha_0 \tilde{P}_0 \int_0^{\tilde{Y}} \mathrm{Ai}\{[\mathrm{i}\alpha_0 U_0'(0)]^{\frac{1}{3}}(\tilde{Y} - \bar{c}_1)\}\,\mathrm{d}\tilde{Y}}{[\mathrm{i}\alpha_0 U_0'(0)]^{\frac{1}{3}}\,\mathrm{Ai}'\{-[\mathrm{i}\alpha_0 U_0'(0)]^{\frac{1}{3}}\bar{c}_1\}}. \tag{8.22}$$

This solution enable us to determine $\Lambda(\hat{c}_1)$ introduced previously,

$$\Lambda = \frac{\alpha_0^2 \int_0^{\infty}\int_{\infty}^{\tilde{Y}} \mathrm{Ai}\{[\mathrm{i}\alpha_0 U_0'(0)]^{\frac{1}{3}}(\hat{Y} - \bar{c}_1)\}\,\mathrm{d}\tilde{Y}\,\mathrm{d}\tilde{Y}}{[\mathrm{i}\alpha U_0'(0)]^{\frac{1}{3}}\,\mathrm{Ai}'\{-[\mathrm{i}\alpha_0 U_0'(0)]^{\frac{1}{3}}\bar{c}_1\}}. \tag{8.23}$$

The procedure is then to determine a solution to (8.11), (8.12) consistent with (8.13), (8.14), and (8.23). However, the problem for $\hat{c}_1$ is highly nonlinear, and as such is a difficult numerical task. However, if we suppose $|\alpha_1| \to \infty$, then

$$\hat{c}_1 = \frac{-\alpha_1 \int_0^1 \hat{R}_3 \hat{p}^+\,\mathrm{d}y}{\int_0^1 [\hat{R}_1 \hat{v}^+ + \hat{R}_2 \hat{p}^+]\,\mathrm{d}y} + O(\alpha^{-\frac{1}{2}}), \tag{8.24}$$

which, on account of the nature of $\hat{p}^+$, $\hat{v}^+$, $\hat{R}_1$, $\hat{R}_2$, $\hat{R}_3$ can be shown to be purely real to leading order; indeed, it is interesting to note that although this system does admit complex values of $\hat{c}_1$ for $\alpha_1 = O(1)$, it appears that the above fails to capture the non-neutral nature of the inviscid modes for $\alpha > \alpha_0$.

However, the reason for this is clearly illustrated by considering the nature of the inviscid system (5.1)–(5.2) in the limit as $\alpha \to \alpha_0$. Suppose that we set

$$\alpha = \alpha_0 + \tilde{\alpha}, \tag{8.25}$$

where

$$|\tilde{\alpha}| \ll |\alpha_0|, \tag{8.26}$$

then we expect expansions of the form

$$\left.\begin{aligned} \tilde{v}_0 &= \hat{v}_0 + \tilde{\alpha}\hat{v}_1 + \tilde{\alpha}^2\hat{v}_2 + O(\tilde{\alpha}^3), \\ \tilde{p}_0 &= \hat{p}_0 + \tilde{\alpha}\hat{p}_1 + \tilde{\alpha}^2\hat{p}_2 + O(\tilde{\alpha}^3), \\ c_0 &= \tilde{\alpha}\hat{c}_1 + \tilde{\alpha}^2\hat{c}_2 + + O(\tilde{\alpha}^3). \end{aligned}\right\} \tag{8.27}$$

The leading-order system is

$$\mathscr{L}_1\{\hat{v}_0, \hat{p}_0\} = 0, \qquad \mathscr{L}_2\{\hat{v}_0, \hat{p}_0\} = 0, \tag{8.28}$$

(see (8.7), (8.9)), with

$$\hat{v}_0(0) = \hat{v}_0(1) = 0. \tag{8.29}$$

At the next order, $\hat{v}_1$ and $\hat{p}_1$ are again determined by means of (8.12), although we shall defer discussion of the boundary conditions to be applied to this system, and turn instead to consideration of the $O(\tilde{\alpha}^2)$ terms. We find

$$\mathscr{L}_1\{\hat{v}_2, \hat{p}_2\} = \frac{U_{0y}\hat{v}_0\hat{c}_1^2}{U_0^3} + \frac{\hat{v}_0 U_{0y}\hat{c}_2}{U_0^2} + \frac{U_{0y}\hat{v}_1\hat{c}_1}{U_0^2} + \frac{\mathrm{i}\hat{p}_1\hat{c}_1}{U_0^2}[T_0 - M_\infty^2 U_0^2]$$

$$+ \frac{\mathrm{i}\hat{p}_0}{U_0^2}\left\{\left[\hat{c}_2 + \frac{\hat{c}_1}{U_0}\right][T_0 - M_\infty^2 U_0^2] + 2M_\infty^2 U_0 \hat{c}_1^2\right\} + 2M_\infty^2 \hat{c}_1\hat{p}_1$$

$$= R_a, \tag{8.30}$$

$$\mathscr{L}_2\{\hat{v}_2, \hat{p}_2\} = -\frac{\mathrm{i}}{T_0}U_0\hat{v}_0 - \frac{2\mathrm{i}\alpha_0}{T_0}U_0\hat{v}_1 + \frac{2\mathrm{i}\alpha_0\hat{c}_1}{T_0}\hat{v}_0 - \frac{\mathrm{i}\alpha_0^2}{T_0}[-\hat{c}_1\hat{v}_1 - \hat{c}_2\hat{v}_0]$$

$$= R_b. \tag{8.31}$$

However, the expansions above are not uniformly valid as $y \to 0$, since $U_0(y) = O(y)$ in this limit, and hence a breakdown to our approximations must occur, specifically when $y = O(\tilde{\alpha})$. If we set

$$y = \tilde{\alpha}\bar{Y}, \quad \bar{Y} = O(1), \tag{8.32}$$

then $\hat{v}_0$ develops in the following manner (that may be demonstrated to be correct *a posterioi*):

$$\hat{v}_0 = \tilde{\alpha}\Phi_0(\bar{Y}) + \tilde{\alpha}^2 \ln\tilde{\alpha}\Phi_1(\bar{Y}) + \tilde{\alpha}^2\Phi_2(\bar{Y}) + \ldots. \tag{8.33}$$

It is simple to show that

$$\Phi_0(\bar{Y}) = -\frac{K_0}{c_1}\bar{Y}, \tag{8.34}$$

where K_0 is some constant; this is consistent with (8.33). We need not consider $\Phi_1(\bar{Y})$ for our purposes, whilst the solution for $\Phi_2(\bar{Y})$ may be written

$$\Phi_2 = \lambda_0 U_0'(0)[U_0'(0)\bar{Y} - \hat{c}_1]\int_0^{\bar{Y}} \frac{\mathrm{d}\bar{Y}}{[U_0'(0)\bar{Y} - \hat{c}_1]} + \ldots \tag{8.35}$$

$$= \lambda_0[U_0'(0)\bar{Y} - \hat{c}_1]\ln\left[\frac{\hat{c}_1 - U_0'(0)\bar{Y}}{\hat{c}_1}\right] + \ldots, \tag{8.36}$$

where we have only retained terms which are of immediate concern and

$$\lambda_0 = \frac{K_0 T_0'(0)}{U_0'(0)T_0(0)} - \frac{U_0''(0)K_0 c_1}{[U_0'(0)]^2} \tag{8.37}$$

The crucial significance of (8.36) is the presence of the $+\mathrm{i}\pi$ jump in the value of the logarithm (Mack 1984, for example), as the point $\bar{Y} = \hat{c}_1/U_0'(0)$ is traversed; it is this that generates an imaginary component to Φ_2, given as $Y \to \infty$ by

$$\Phi_2^i \sim \lambda_0\pi[U_0'(0)\bar{Y} - c_0], \tag{8.38}$$

(here and below a superscript 'i' denotes an imaginary component).

Returning to our discussion of the core region, we see we must have that

$$\hat{v}_1(0) = \hat{v}_1(1) = 0, \tag{8.39}$$

and consequently $\hat{c}_1$ is determined by (8.14), with $A = 0$. On account of the nature of $\hat{R}_1$, $\hat{R}_2$, $\hat{R}_3$, $\hat{v}^+$, $\hat{p}^+$ we expect $\hat{c}_1$ to be a *real* quantity.

We are now in a position to specify the following boundary conditions:

$$\hat{v}_2(1) = 0, \quad \hat{v}_0^i(0) = -\lambda_0 \hat{c}_1 \pi, \tag{8.40}$$

and thus $\hat{c}_2^i$ may be determined, in principle, by means of the conditions

$$\int_0^1 [R_a^r \hat{v}^+ + R_b^i p^+] \, \mathrm{d}y = \hat{v}(0) \lambda_0 \hat{c}_1 \pi, \tag{8.41}$$

where superscript 'r' denotes a real part.

Unfortunately, we see from (8.37) that λ_0 is dependent upon $T_0'(0)$ and $U_0''(0)$, and since both these quantities are zero in the case of an adiabatic lower wall, then in this case we must consider (8.27) up to $O(\tilde{\alpha}^3)$ in order to determine a value for the imaginary component of the wave speed as $\tilde{\alpha} \to 0$; however, since the general technique is well established above, we do not carry this out in this paper.

The key result, therefore, is then that $\mathrm{Im}\{c_0\}$ is $O(\tilde{\alpha}^2)$ in general (but $O(\tilde{\alpha}^3)$ in the insulated wall case), and as a consequence we do not expect to obtain non-neutral values of $\hat{c}_1$ from (8.14) as $\alpha_1 \to \infty$ (this would only be expected in a study of the $O(\epsilon^2)$ terms of the c-expansion, in general, and the $O(\epsilon^3)$ terms in the case of an insulated lower wall). Indeed, the two expansions in this section, namely (8.1) and (8.25) are equivalent in many ways, notably as $|\alpha_1| \to \infty$. The above also clearly illustrates how c_0 is only complex for values of $\alpha > \alpha_0$, since for $\alpha < \alpha_0$ the 'jump' in the value of the logarithm is not present.

9. A change of boundary conditions

It is interesting that the (confined) flow profile under consideration in this paper has such different stability characteristics from those of the (external) boundary layer. This leads us to question the nature of these fundamental differences.

One obvious candidate for investigation is the effect of the boundedness of the domain (i.e. the impermeability condition imposed on *two* walls). In an attempt to assess this effect, we considered the problem where the impermeability constraint on the upper wall ($y = 1$) is replaced by one of radiation, while retaining the same basic profile. Specifically, we replace (5.3) by

$$\tilde{v}_0(0) = 0 \tag{9.1}$$

(as before), but with

$$\frac{\partial \tilde{v}_0}{\partial y} + \nu \tilde{v}_0 = 0 \quad \text{on} \quad y = 1, \tag{9.2}$$

where

$$\nu = \pm \alpha [1 - M_\infty^2 (1 - c_0)^2]^{\frac{1}{2}}. \tag{9.3}$$

Here the sign of ν is chosen to ensure that $\mathrm{Re}\{\nu\} > 0$. Indeed, this amounts to considering the piecewise-continuous flow which consists of our basic Couette flow for $0 \leqslant y < 1$ and uniform flow ($U_0(y) = T_0(y) = 1$) over $1 < y < \infty$. This may be shown using the arguments used by Drazin & Reid (1981) who considered incompressible piecewise-linear velocity profiles and imposed continuity of pressure at $y = 1$.

The system defined by (5.1)–(5.2), (9.1)–(9.2) is solved numerically by the techniques used in obtaining the results of §6 (i.e. a Runge–Kutta shooting scheme in conjunction with a Newton iteration scheme to iterate on c_0).

Results for one example were obtained, namely for $M_\infty = 2$, with adiabatic conditions on the temperature at $y = 0$. Results for $\mathrm{Re}\{c_0\}$ are shown in figure 16(*a*).

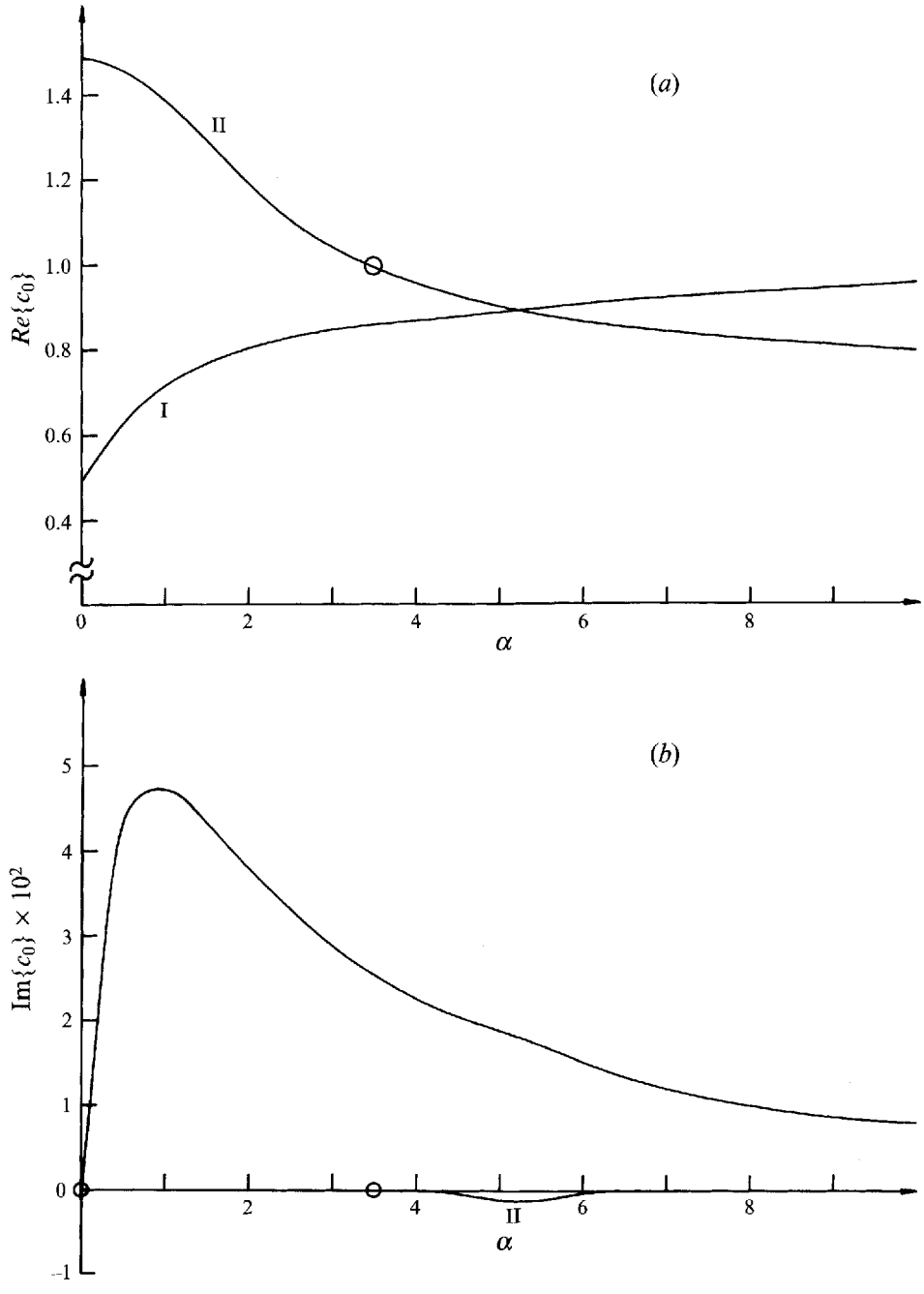

FIGURE 16. (*a*) $\mathrm{Re}\{c_0\}$ and (*b*) $\mathrm{Im}\{c_0\}$ as a function of α for $M_\infty = 2$, radiation boundary condition on $y = 1$.

Two modes were found, the first (mode I) originates at $\alpha = 0$, with a wave speed $c_0 = 1 - 1/M_\infty = 0.5$, and as such is typical of so-called 'first modes' observed in supersonic boundary-layer stability studies (e.g. Mack 1987). Mode II, on the other hand, originates with a wave speed $c_0 = 1.50$, and consequently is more typical of the bounded-flow modes observed in previous sections of this paper. Figure 16(*b*) shows

the variation of $\mathrm{Im}\{c_0\}$ with α. Mode I is unstable over the entire range of α shown, while mode II is neutrally stable up to $\alpha \approx 3.5$, at which point $\mathrm{Re}\{c_0\}$ drops below unity, and $\mathrm{Im}\{c_0\}$ becomes negative, indicating a stable mode. We were unable to find other modes over the range of α considered, particularly modes with $\mathrm{Re}\{c_0\} < 0$, although it is very likely that such modes exist, particularly at larger values of α. Thus it appears that the imposition of radiation-type boundary conditions results in a hybrid situation, with stability characteristics similar to those found in both bounded and unbounded flows.

10. Conclusions

In this paper we have considered the linear stability of compressible plane Couette flow. Our numerical results for the full governing equations are clearly in agreement with the predictions of Morawetz (1952, 1954) regarding the structure of the spectrum. The main thrust of this paper has been directed towards modes which have been predominantly inviscid in nature. It appears that these are the most important, since they may become unstable, while our studies indicate that viscosity plays a generally stabilizing role, throughout. Although we have computed the spectrum of eigenmodes from the linearized Navier–Stokes equations for extremely high Reynolds numbers, we have not found evidence of unstable modes (at least to $M_\infty = 5$). This is not inconsistent with the inviscid results, although we would expect to find unstable modes when viscous effects are taken into account if they are sufficiently small.

The expansions of the assumed form (4.14) are typical of solutions which are predominantly inviscid, but have viscous corrections (see also Morawetz 1952). In §8 we studied the important regimes where $c_0 \to 0$ (or $c_0 > 1$) in which the first two terms in the series become comparable, a critical layer forms close to one of the walls, and the viscous layer thickens to $O(Re^{-\frac{1}{3}})$. These are the 'exceptional' cases referred to by Morawetz (1952).

In §9, it was show how, to a large extent, it is the boundary conditions imposed on disturbances, that determine the nature of the stability of the flow. Indeed, earlier in the paper, in §4 it was shown in the study of the GIP condition that it is important to impose correct (i.e. radiation type) boundary conditions in the case of unbounded flows to avoid the (erroneous) requirement that a GIP is necessary for the existence of supersonic neutral modes.

This work was supported by the National Aeronautics and Space Administration under NASA contract NAS1-18605 while the authors were in residence at the Institute for Computer Applications in Science and Engineering (ICASE), NASA Langley Research Center, Hampton. This work was also supported by the SERC. The authors wish to thank the referees for a number of insightful comments.

REFERENCES

ASHPIS, D. E. & ERLEBACHER, G. 1990 On the continuous spectra of the compressible boundary layer stability equations. In *Instability and Transition II* (ed. M. Y. Hussaini & R. G. Voigt), p. 145. Springer.

BALSA, T. F. & GOLDSTEIN, M. E. 1990 On the stability of supersonic mixing layers: A high Mach number asymptotic theory. *J. Fluid Mech.* **216**, 585.

BLACKABY, N., COWLEY, S. J. & HALL, P. 1993 On the instability of hypersonic flow past a flat plate. *J. Fluid Mech.* **247**, 369. (Also *ICASE Rep.* 90–40.)

CASE, K. M. 1960 Stability of the inviscid plane Couette flow. *Phys. Fluids* **3**, 143.

CASE, K. M. 1961 Hydrodynamic stability and the inviscid limit. *J. Fluid Mech.* **10**, 420.

COWLEY, S. J. & HALL, P. 1990 On the instability of hypersonic flow past a wedge. *J. Fluid Mech.* **214**, 17.

DAVEY, A. 1973 On the stability of plane Couette flow to infinitesimal disturbances. *J. Fluid Mech.* **57**, 369.

DEARDORFF, J. W. 1963 On the stability of viscous plane Couette flow. *J. Fluid Mech.* **15**, 623.

DIKII, L. A. 1964 On the stability of plane-parallel Couette flow. *Prikl. Mat. Mekh.* **28**, 389. (Transl. in *J. Appl. Math. Mech.* **28**, 1009 (1965).)

DRAZIN, P. G. & REID, W. H. 1981 *Hydrodynamic Stability*. Cambridge University Press.

DUCK, P. W. 1990 The inviscid axisymmetric stability of the supersonic flow along a circular cylinder. *J. Fluid Mech.* **214**, 611.

ECKAUS, W. 1965 *Studies in Nonlinear Stability Theory*. Springer.

ELLINGSEN, T., GJEVIK, B. & PALM, L. 1970 On the non-linear stability of plane Couette flow. *J. Fluid Mech.* **40**, 97.

GAJJAR, J. S. B. 1990 Amplitude-dependent neutral modes in compressible boundary layer flows. In *Proc. Workshop on Instability and Transition* (ed. M. Y. Hussaini & R. G. Voigt), vol. 1, p. 40. Springer.

GAJJAR, J. S. B. & COLE, J. W. 1989 The upper-branch stability of compressible boundary-layer flows. *Theor. Comput. Fluid Dyn.* **1**, 105.

GALLAGHER, A. P. 1974 On the behavior of small disturbances in plane Couette flow. Part 3. The phenomena of mode-pairing. *J. Fluid Mech.* **65**, 29.

GALLAGHER, A. P. & MERCER, A. 1962 On the behavior of small disturbances in plane Couette flow. *J. Fluid Mech.* **13**, 91.

GALLAGHER, A. P. & MERCER, A. 1964 On the behavior of small disturbances in plane Couette flow. Part 2. The higher eigenvalues. *J. Fluid Mech.* **18**, 350.

GIRARD, J. J. 1988 Study of the stability of compressible Couette flow. PhD dissertation, Washington State University.

GLATZEL, W. 1988 Sonic instability in supersonic shear flows. *Mon. Not. R. Astron. Soc.* **233**, 795.

GLATZEL, W. 1989 The linear stability of viscous compressible plane Couette flow. *J. Fluid Mech.* **202**, 515.

GOLDSTEIN, M. E. & WUNDROW, D. W. 1990 Spatial evolution of nonlinear acoustic mode instabilities on hypersonic boundary layers. *J. Fluid Mech.* **219**, 585.

GREENOUGH, J., RILEY, J. J., SOETRISMO, M. & EBERHARDT, S. 1989 The effects of walls on a compressible mixing layer. *AIAA Paper* 89-0372.

GROHNE, D. 1954 Uben das Spektrum bei Eigenschwingangen ebienen Laminurströmungen. *Z. Angew. Math. Mech.* **34**, 344. (Transl. in *Tech. Mem. Natl Adv. Commun. Aero. Wash.*, No. 1417 (1957).)

HAINS, F. D. 1967 Stability of plane Couette–Poiseuille flow. *Phys. Fluids* **10**, 2079.

HERBERT, T. 1990 A code for linear stability analysis. In *Instability and Transition I* (ed. M. Y. Hussaini & R. G. Voigt), p. 121. Springer.

JACKSON, T. & GROSCH, C. E. 1989 Inviscid spatial stability of a compressible mixing layer. *J. Fluid Mech.* **208**, 609.

LEES, L. & LIN, C. C. 1946 Investigation of the stability of the laminar boundary layer in a compressible fluid. *NACA Tech. Note* 1115.

LESSEN, M. & CHEIFETZ, M. G. 1975 Stability of plane Couette flow with respect to finite two-dimensional disturbances. *Phys. Fluids* **18**, 939.

LIN, C. C. 1955 *The Theory of Hydrodynamic Stability*. Cambridge University Press.

MACARAEG, M. G. & STREET, C. L. 1989 New instability modes for bounded free stream flows. *Phys. Fluids* A **1**, 1305.

MACK, L. M. 1963 The inviscid stability of the compressible laminar-boundary layer. In *Space Programs Summary No.* 37–23, p. 297. J.P.L., Pasadena, CA.

MACK, L. M. 1965*a* Stability of the compressible laminar boundary layer according to a direct numerical solution. *AGARDograph* 97, Part 1, p. 329.

MACK, L. M. 1965*b* Computation of the stability of the laminar boundary layer. In *Methods in Computational Physics* (ed. B. Adler, S. Fernbach & M. Rotenberg), Vol. 4, p. 247. Academic.

MACK, L. M. 1969 Boundary-layer stability theory. *Document No.* 90-277, Rev. A. J.P.L., Pasadena, CA.

MACK, L. M. 1984 Boundary-layer linear stability theory. *AGARD Rep.* 704, 3-1.

MACK, L. M. 1987 Review of compressible stability theory. In *Proc. ICASE Workshop on the Stability of Time Dependent and Spatially Varying Flows*, p. 164. Springer.

MACK, L. M. 1990 On the inviscid acoustic-mode instability of supersonic shear flows. Part 1. Two dimensional waves. *Theor. Comput. Fluid Dyn.* **2**, 97.

MILES, J. W. 1961 On the stability of heterogeneous shear flows. Part 2. *J. Fluid Mech.* **16**, 209.

MORAWETZ, C. S. 1952 The eigenvalues of some stability problems involving viscosity. *J. Rat. Mech. Anal.* **1**, 579.

MORAWETZ, C. S. 1954 Asymptotic solutions of the stability equations of a compressible fluid. *J. Maths Phys.* **33**, 1.

PAPAGEORGIOU, D. 1990 Linear stability of the supersonic wave behind a flat plate aligned with a uniform stream. *Theor. Comput. Fluid Dyn.* **1**, 327.

REDDY, S. C., SCHMID, P. J. & HENNINGSON, D. S. 1993 Pseudospectra of the Orr–Sommerfeld operator. *SIAM J. Appl. Maths* **53**, 15.

REICHARDT, H. 1956 Üben die Geschwindigkeitsverteilung in einer geradlinigen turbulenten Couetteströmung. *Z. Angew. Math. Mech.* **36**, 526–529.

REID, W. H. 1979 An exact solution of the Orr–Sommerfeld equation for plane Couette flow. *Stud. Appl. Maths* **4**, 83.

RESHOTKO, E. 1962 Stability of three-dimensional compressible boundary layers. *NASA Tech. Note* D-1220.

RESHOTKO, E. 1976 Boundary layer stability and transition. *Ann. Rev. Fluid Mech.* **8**, 311.

REYNOLDS, W. C. & POTTER, M. C. 1967 Finite-amplitude instability of parallel shear flows. *J. Fluid Mech.* **27**, 465.

ROBERTSON, J. M. 1959 On turbulent plane-Couette flow. In *Proc. 6th Mid. Western Conf. on Fluid Mech., University of Texas*, p. 169.

ROMANOV, V. A. 1973 Stability of plane-parallel Couette flow. *Funkcional Anal. i Prolożen.* **7**, No. 2, 62. (Transl. in *Functional Anal. Applics.* **7**, 137 (1973).)

SHIVAMOGGI, B. K. 1982 Stability of inviscid plane Couette flow. *Acta Mechanica* **44**, 327.

SMITH, F. T. & BROWN, S. N. 1990 The inviscid instability of a Blasius boundary layer at large values of the Mach number. *J. Fluid Mech.* **219**, 499.

STEWARTSON, K. 1981 Marginally stable inviscid flow with critical layers. *IMA J. Appl. Maths* **27**, 133.

SYNGE, J. L. 1938 Hydrodynamical stability. *Semi-Centenn., Publ. Amer. Math. Soc.* **2**, 227.

TAM, C. K. W. & HU, F. Q. 1989*a* On the three families of instability waves of a high-speed jets. *J. Fluid Mech.* **201**, 447.

TAM, C. K. W.& HU, F. Q. 1989*b* The stability and acoustic wave nodes of supersonic mixing layers inside a rectangular channel. *J. Fluid Mech.* **203**, 51.

TAYLOR, G. I. 1936 Fluid friction between rotating cylinder. *Proc. R. Soc. Lond.* A **157**, 546.

WASOW, W. 1953 On small disturbances of plane Couette flow. *J. Res. Natl Bur. Stand.* **51**, 195.

WATSON, J. 1960 On the non-linear mechanics of wave disturbances in stable and unstable parallel flows. Part 2. The development of a solution for plane Poiseuille flow and for plane Couette flow. *J. Fluid Mech.* **9**, 371.

ZHUANG, M., KUBOTA, T. & DIMOTAKIS, P. E. 1990 The effect of walls on a spatially growing supersonic shear layer. *Phys. Fluids* A **2**, 599.